Systematic losses in tree-canopy cover over three decades revealed by integrating complementary data sources

Authors

Ruben Remelgado[1]*, Carsten Meyer[1,2,3*]

Affiliations

1. Macroecology & Society, German Centre for Integrative Biodiversity Research (iDiv), Halle-Leipzig-Jena, Deutscher Platz 5e, 04103 Leipzig, Germany

2. Institute of Geosciences and Geography, Martin Luther University Halle-Wittenberg, Halle (Saale), Germany.

3. Institute of Biology, Leipzig University, Leipzig, Germany

*co-corresponding author(s): Ruben Remelgado (ruben.remelgado@idiv.de; ORCID ID: 0000-0002-9871-5703) and Carsten Meyer (carsten.meyer@idiv.de; ORCID ID: 0000-0003-3927-5856)

ABSTRACT

Losses and gains in canopy cover of the world's tree canopies affect carbon stocks, species habitats, water cycles, and human livelihoods. Consistent and multi-decadal global data on tree-canopy cover dynamics are needed for modelling climate scenarios, tracking progress towards restoration targets, and diverse other research, management and policy applications. However, most data only map binary 'forest'/'non forest' distinctions that are regionally restricted or biassed by data gaps, and those mapping tree-canopy cover are limited to the 21st century, leaving longer-term dynamic in tree-canopy cover largely unknown. Here, we present an annual and global time-series of tree-canopy cover between 1992 and 2018. To develop these data, we integrated complementary products, using their respective strengths to compensate for weaknesses, and exploiting path dependencies in change processes to derive predictions into the data-sparse 1990s. Our model validation indicates we can accurately map tree-canopy cover (r^2=0.95 [±0.01], RMSE=6.75% [±0.08], F1-score=0.97 [< ±0.01]) and our time-series show plausible broad-scale spatiotemporal patterns, as indicated by high correlations with national statistics (r^2=0.94 [< ±0.01]). Our analysis of these data revealed systematic global losses in tree-canopy cover that, area-wise, substantially exceed concurrent losses or gains of treescape extents. Our analysis and data provide novel insights into global dynamics of tree cover, and can support modelling and

reporting in the scope of the Kunming-Montréal Global Biodiversity Framework, the Paris Agreement, and other forest-related policies.

INTRODUCTION

Global dynamics in tree-canopy cover, resulting from changes in the densities, extents, and fragmentation of tree stands, have diverse impacts on Earth's biota and earth-system processes. Thinning tree canopies affect biogeochemical cycles directly by reducing carbon stores (Baul et al., 2021; L. Xu et al., 2018), and indirectly by increasing tree exposure to wind and solar radiation, thereby increasing their susceptibility to drying, fire, and subsequent carbon losses (Walker et al., 2019). Tree-canopy cover dynamics also affect biodiversity by altering resources available to different species (e.g., shelter, food) and the microclimatic conditions to which they are exposed (Kašpar et al., 2021). Simultaneously, tree-canopy cover changes variously affect humans via effects on surface-water run-off (Selbig et al., 2022), soil erosion (Mohammad and Adam, 2010), crop pollination (Krishnan et al., 2020), urban heat islands (Schwaab et al., 2021), mental health (Lee et al., 2023), and real estate values (Kovacs et al., 2022).

Correspondingly, consistent historical data on the spatiotemporal dynamics of tree-canopy cover are needed to inform actions towards multiple goals and targets under the 2030 Agenda for Sustainable Development (Estoque et al., 2021) For example, long time-series of tree-canopy cover can support climate policy by enabling the modelling of future scenarios (Allen et al., 2017) and definitions of Nationally Determined Contributions to the Paris Agreement (UNFCCC, 2015). Similarly, long time-series help assess changes in forests and other wooded ecosystems since 1990, which is a globally adopted reference year for cutting greenhouse gas emissions (Kuyper et al., 2018).

Thanks to technical advances and capacity-building investments over recent decades, remote sensing increasingly offers cost-effective solutions to support spatiotemporal data requirements on key properties of global woodlands (Cameron et al., 2019), including on tree-canopy cover. Yet, existing global data on long-term tree-canopy cover dynamics are available only at coarse spatial resolutions (Song et al., 2018), with intermediate- and high-resolution products limited to post-2000 and post-2015 periods, respectively, or single years before then (Dimiceli et al., 2015; Sexton et al., 2013, Hansen et al., 2013; Tang et al., 2019).

In turn, global remote sensing products extending to earlier years map binary forest/non-forest distinctions. Those products rely on "forest" definitions based on thresholds of tree-canopy cover (e.g., between 10 and 70 percent, alongside other criteria; (Chazdon et al., 2016)), which hinders the comparability of change reports enabled by different products. Moreover, there are risks of misinterpreting change magnitudes when using categorical products to analyse forest changes, which are often slow and progressive, as any change detection depends on crossing a specific threshold in either direction (Montibeller et al., 2020).

Deriving a global and dense time-series of tree-canopy cover requires surpassing satellite data limitations. For half a century, Landsat became a popular data source for historical forest-mapping thanks to its global coverage and high spatial and temporal resolution (Hansen et al., 2013; Kim et al., 2014; Vancutsem et al., 2021). However, the Landsat archive suffers from multi-year data gaps that limit consistent, global environmental monitoring (Remelgado et al., 2023). Consequently, existing products extending into the 1990s (all of which, to the best of our knowledge, tackle forest cover and not tree-canopy cover) are incomplete (Kim et al., 2014), focused on specific countries (Cohen et al., 2010; Lehmann et al., 2015; MapBiomas, 2021; Stibig et al., 2014; Wulder et al., 2020) or biomes (Vancutsem et al., 2021), or provide biassed perceptions of change due to gradual improvements in satellite data coverages (Remelgado et al., 2023). Alternatively, to Landsat, AVHRR data offers a mostly consistent temporal and spatial coverage since the 1980s that enabled mapping long-term tree-cover changes (Song et al., 2018). Yet, its 5-km spatial resolution is too coarse to monitor forest changes reliably, given that those commonly occur at finer scales (Montibeller et al., 2020).

Predictive models that integrate heterogeneous data with support of covariates provide a unique opportunity to tackle these data limitations. Such models can capitalise on the ability of different remote-sensor systems and mapping algorithms to perceive different facets of forest dynamics (Wang et al., 2020). Model-based data integration can borrow information across spatial and temporal scales, building on the facts that local forest dynamics are characterised by path-dependent processes (Montibeller et al., 2020; Taubert et al., 2018), and that change dynamics are influenced by cross-scale interactions (Soranno et al., 2014, **Fig. 1**). For example, although gaps in satellite imagery hamper direct fine-scale mapping of forest-change processes pre-2000, data for later years may still bear signals of earlier dynamics, and thus help reveal longer-term changes. Similarly, consistent coarser-resolution observations over longer periods capturing historical changes across larger landscapes may help determine the timing, direction, and magnitude of fine-scale changes. Yet, the potential of model-based data integration for global time-series mapping remains underutilised. Correspondingly, global, long-term dynamics of tree-canopy cover at sub-kilometre resolutions remain largely unknown.

Here, we leveraged these concepts by integrating state-of-the-art and high-resolution gridded data on tree-canopy cover and tree-cover losses (Hansen et al., 2013) with that on tree-canopy cover change - and drivers of that change - mapped at coarser spatial resolutions. The result is the Global Tree-Canopy Cover Change dataset (GTCCC), a global time-series of tree-canopy cover and change between 1992 and 2018 mapped annually at a 300-m resolution. We use this synthesis product to analyse longer-term historical dynamics of tree-canopy cover, providing novel insights into their timing and speed, as well as into the magnitude, direction, and generality of net chances.

MATERIALS AND METHODS

Overview of modelling strategy

We mapped global tree-canopy cover using a machine-learning framework (**Fig. 1**) that exploits the fact that trajectories of forest persistence and change are commonly path-dependent (Montibeller et al., 2020; Taubert et al., 2018). This allows us to predict tree-canopy cover in the 1990s when high-resolution data is lacking, and consistently thereafter.

Our modelling framework uses higher-resolution data on tree-canopy cover as both a source of samples and as a predictor. These data inform on the outcome of long-term tree-canopy cover changes in a future reference year (T), and are obtained from a dataset available only since the year 2000 (see **Fine-scale tree-canopy cover**). For each mapping year (t), which span from 1992 to 2018, we instead used coarser-resolution data on environmental drivers of tree-canopy cover change (**Table 1 of SI**). This includes data on land-cover (see **Land cover**), vegetation continuous fields (see **Coarse-**

resolution vegetation dynamics), human settlements and political boundaries (see **Human factors**), and climate and topography (see **Environmental drivers of tree growth**).

Furthermore, our modelling framework explicitly accounts for change dynamics. For this, we included data on the direction and magnitude of changes between years t and T (see **Coarse-resolution vegetation dynamics**), as well as data on fine-scale tree-canopy cover gains and losses by between 2000 and 2019 (the period for which our reference data is available, see **Fine-scale tree-canopy cover**). In addition, we included a dummy variable on the number of years between the years t and T to control for fixed temporal effects and temporal path-dependencies.

Finally, our modelling framework includes data on the (dis)agreement between inputs that measure (or are sensitive to) tree-canopy cover (see **Cross-scale perceptions of tree-canopy cover**). This to synthesise perceptions of tree-canopy cover, allowing us to exploit the strengths and weaknesses of individual data products.

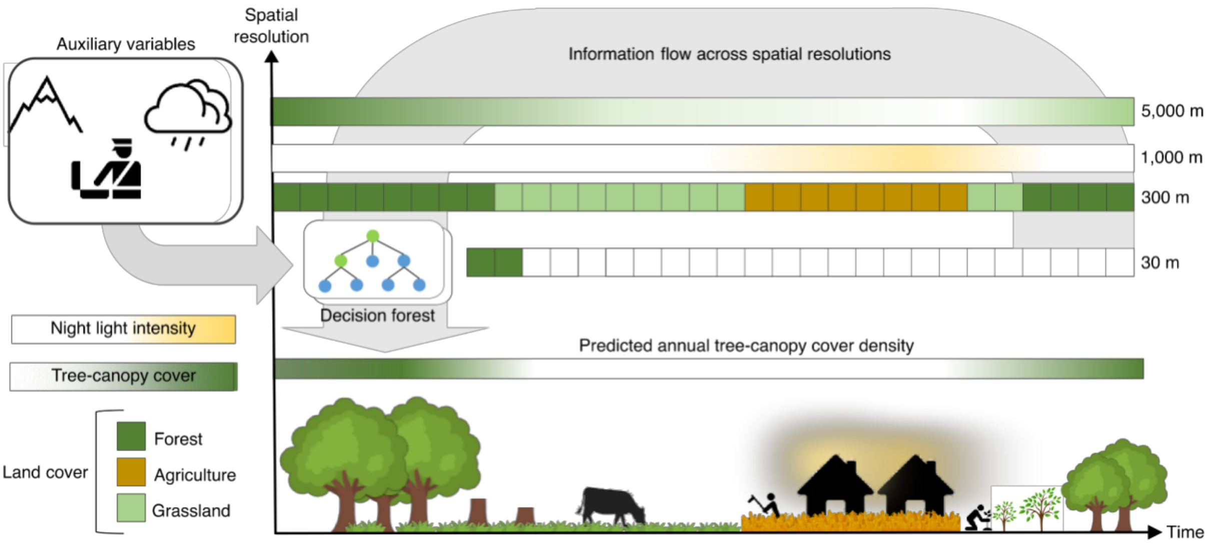

Figure 1 – Conceptual overview of our modelling framework. The model aims to reconstruct historical dynamics of continuous tree-canopy cover at 300-m resolution. To capture signals of the true change trajectories (e.g., the iconized example), the model integrates high-resolution, but temporally incomplete data on tree-canopy cover with coarser-resolution data on categorical land cover, continuous canopy cover dynamics, night-lights, and auxiliary data (topography, climate, political boundaries). The model learns about interactions among variables across spatial grains, spatiotemporally varying strengths and weaknesses of coarser-grain products, and temporal path-dependencies of fine-grain change processes captured only in later years, and uses the learned information for its annual predictions.

Modelling framework

We modelled tree-canopy cover with Random Forest Regression (RFReg, Breiman, 2001) as implemented in Python's Scikit-learn module (Pedregosa et al., 2011). The algorithm constructs multiple decision trees (i.e., a "forest"), each of which with its own decision path to the tree-canopy cover values reported in the training data. When applying the RFReg model to each pixel in a regular spatial grid, and in each prediction year, the different decision trees estimate a tree-canopy cover value, and the estimates of all trees are averaged into a final prediction.

We trained our model with 180 trees (hereafter referred to as "forest size"). To determine this number, for each of 10 runs, we extracted a random subset of 10,000 samples to test how forest sizes between 40 and 500 trees, in intervals of 20, led to gains in model performance (**Fig. 1a of SI**). At each iteration, we built a RFReg model and recorded its Out-Of-Bag (OOB) score, which corresponds to the coefficient of determination (r^2) between the in-bag and out-of-bag samples. After all iterations, we calculated the mean OOB value at each forest size, and used Python's Kneed module (Satopaa et al., 2011) to find the start of a plateau in performances where increases in forest sizes did not improve accuracies noticeably (i.e., the 'knee' of the distribution).

Prediction uncertainties

We estimated the 95% Confidence Intervals (CI) across the predictions of all decision trees for each pixel and year combination. This was calculated as 196*SE, where the Standard Error (SE) is calculated as the standard deviation of the predictions, divided by the square root of the forest size. We used the CI to derive upper and lower confidence bounds around the average estimate for each pixel and year. We used these bounds to associate our subsequent assessments with uncertainty bounds (see **Change analysis** and **Comparison with national statistics**).

Sampling

We informed our model with samples from a high-resolution dataset that offers the most reliable global reference on tree-canopy cover (see **Fine-scale tree-canopy cover**). We sampled on a country-by-country basis, thereby accounting for likely differences in forest-management regimes across political boundaries (Herrera et al., 2019). Here, we treated any non-contiguous land masses of a given country separately, resulting in 114,020 sampling units. For example, we treated the conterminous USA as a single unit, and addressed Alaska and each Hawaiian island separately, therefore ensuring sampling across unique environmental/management contexts.

For each country (referred hereafter as a 'region of interest', or roi), we stratified our sampling based on land-cover. Doing so ensured the collection of samples from every category, tackling the inability of RFReg to predict out-of-sample. In a given roi, the number of samples per class was estimated as $n_{roi}\,\Sigma(p_j = c)/n_c$, where n_c is the total number of pixels of the target class, p_j is the target pixel at position j, and n_{roi} is the total number of samples to be extracted within the roi. The value n_{roi} was estimated as being at least one sample per 150x150 pixels (i.e., 50-km^2 at the equator). This value was determined empirically as a compromise between model accuracy and computational intensity.

In a given roi, for each class c, we sampled half of the estimated n_c randomly over pixels where our reference data did not detect changes in tree-canopy cover between 2000 and 2018. We collected the remaining half over pixels with changes, where we applied a skewness-adjusted random-sampling approach. Here, we calculated the skewness of the change distribution. Then, we used the inverse of the shape parameter to build a skewed sampling distribution to guide the random selection of samples. We calculated the skewed distribution with NumPy's skewnorm function (Harris et al., 2020).

This skewness-adjusted sampling tackles the potential rarity of changes at the upper and lower edges of the change distribution. For example, in a roi where smaller changes are dominant, the distribution will become left-skewed. Here, non-probabilistic random sampling would privilege smaller changes, creating an imbalanced sample set. This would negatively impact RFReg by restricting its predictive capabilities to a narrow range of outcomes.

Note that the sampling based on tree-canopy cover changes disregards pixels experiencing gains. This is because gains are mapped in the reference dataset as a mask of occurrences between 2000 and 2012. Therefore, it is not possible to infer the true year of change. Nonetheless, our goal is to map year-specific values of tree-canopy cover and not change percentages. This filtering merely controls for sample quality, and does not limit our ability to predict gains thereafter.

We collected 78,135 sampling locations (**Fig. 1b of SI**). At each location, we sampled tree-canopy cover on an annual basis from 2000 to 2008, resulting in a training set of 625,080 samples, and accordingly extracted all predictor variables. We then used these data to train a model predicting annual tree-canopy cover densities (see **Overview of modelling strategy**).

Predictors

Fine-scale tree-canopy cover

For each year for which we mapped tree-canopy cover, our modelling framework uses a later reference on that variable that informs on the outcome of long-term changes. Here, we constructed annual layers on tree-canopy cover, from 2000 to 2019, using the Global Forest Change dataset (GFC, version 1.8, Hansen et al., 2013). Specifically, we used 30-m data on tree-canopy cover mapped for 2000, and extended it annually by disaggregating associated data on the year of tree-canopy cover losses. For each pixel and year combination, we preserved the tree-canopy cover value of year 2000 until the loss year, at which point we updated the baseline value to 0% following the definition of a loss given by the authors. Then, we discarded pixels with < 10% tree-canopy cover due to reportedly high likelihoods of false detections of sparse tree-cover with Landsat imagery (Achard et al., 2014). Finally, we aggregated the annual layers via averaging to our target mapping resolution of 300-m.

In addition to data on tree-canopy cover changes, we accounted for changes in this variable at different spatial scales to account for spatial contagions (Ferrer Velasco et al., 2020; Rosa et al., 2013). Here, we derived two predictors. Firstly, we calculated the density of 30-m pixels nested within a 300-m pixel that experienced a loss at any point during the 2000-2019 period. Secondly, we calculated the average temporal distance of loss years relative to 2000. We produced both variables at our mapping resolution of 300-m and, additionally, at a 5-km resolution with respect to the coarsest data used in this study (see **Coarse-resolution vegetation dynamics**).

Coarse-resolution vegetation dynamics

We used AVHRR-based Vegetation Continuous Fields data (AVHRR-VCF, Song et al., 2018), which map per-pixel percentages of tree cover (taller than 5 m), short vegetation, and non-vegetated surfaces between 1982 and 2016. Due to its relatively high global and temporal consistency, these data allow us to describe regional vegetation dynamics, and provide our modelling framework with information on temporal path-dependencies.

The AVHRR-VCF data end in 2016, and we could not extend them with the original methods due to the degradation of AVHRR sensors (Dech et al., 2021). Instead, we extended these data with that of the Copernicus land cover dataset (CLC, Buchhorn et al., 2020), which maps per-pixel proportions of 9 land-cover classes between 2015 and 2019 at a 100-m resolution. To match these data to the lower thematic and spatial resolution of the AVHRR-VCF data, we aggregated the CLC data by summing proportions of land-cover classes into AVHRR-VCF categories and averaged them to a 5-km resolution. A description of the modelling framework and the corresponding outputs can be found in a dedicated repository (https://doi.org/10.5281/zenodo.8217455).

We used the extended AVHRR-VCF time-series to derive predictor variables on percent changes. For each pixel and year, we estimated changes in relation to the nearest future year with available GFC data. For example, changes from 1992 onwards were calculated in comparison to the year 2000. In turn, changes from the year 2000 were estimated in comparison to data from the year 2001.

Land cover

We integrated annual data on the dominant land cover in 300-m-resolution pixels (distinguishing 38 land-cover/use classes following the UN Land Cover Classification System; **Table 2 of SI**), as mapped by the Climate Change Initiative Land Cover dataset (CCILC, Santoro et al., 2017).

Categorical land-cover data aids predictions of tree-canopy cover in several ways. First, the class distinctions indicate whether or not tree-cover is perceived as the dominant land cover. Second, even if land-cover classifications face persistent regional issues, they can still carry relevant signals that help a model make more accurate predictions. This is because the spatial configurations of (correctly or falsely) perceived tree-cover classes, and also those of other land-cover classes that are easily confused with tree-cover (e.g., shrubland), often follow true gradients of either tree-canopy cover or of canopy-cover-affecting environmental conditions or management regimes.

Cross-scale perceptions of tree-canopy cover

We mapped tree-canopy cover at a 300-m resolution, but we lack such fine scale data throughout our mapping period. To tackle this issue, we included several other datasets that either directly map or are sensitive to this variable, and that provide consistent, annual information. Given these data result from different modelling strategies, they show disagreements. Yet, these disagreements provide varying perceptions that help complement the weaknesses of individual products.

We derived predictors on the differences in mapped tree-canopy cover densities between the CCILC, AVHRR-VCF, and GFC datasets. We computed the percent differences of each combination of the aforementioned datasets at a 5-km resolution, with respect for the lowest resolution dataset (i.e., AVHRR-VCF). For the comparison between the AVRR-VCF and CCILC datasets, we estimated annual differences from 1992 and 2018. For the comparison of both AVHRR-VCF and CCILC with the GFC, we estimated annual differences between 2000 and 2019. Because the CCILC dataset is categorical, we translated land-cover classes into tree-canopy cover Following similar past experiments (Song et al., 2014), we estimated that classes occupy the central percentage value of the range of possible values indicated in their respective labels (**Table 2 of SI**).

Environmental drivers of tree growth

We integrated predictor variables to account for the driving influence of topography and climate on global tree abundances (Crowther et al., 2015). Firstly, elevation drives spatial variation in forest structure (Mazón et al., 2020), whereas slope influences both natural (e.g., landslides, Maraun et al., 2022) and human drivers of tree-canopy cover changes (e.g., feasibility of industrial logging, FAO, 1998). Therefore, we obtained layers on elevation and slope from a 90-m-resolution digital elevation model (Yamazaki et al., 2017), and averaged them to our 300-m mapping resolution. Secondly, tree-growth is strongly determined by water availability and its seasonality (X. Xu et al., 2018). Therefore, we derived data on the annual total precipitation (P) and Aridity Index (AI, Barrow, 1992) based on monthly precipitation (P) and potential evapotranspiration (PET) data from the 1-km CHELSA dataset (version 2.0, Karger et al., 2017). Whereas P indicates the presence and abundance of available water, the AI, estimated for each year t as $\sum_{t=1}^{n} P_t / \sum_{t=1}^{n} PET_t$, serves as a proxy for water seasonality and scarcity. When the AI is 0, this indicates the absence of water, or its rapid evaporation due to high temperatures. In turn, when the AI is high (generally above 1), precipitation is higher than PET, indicating moist conditions. In addition, when a higher P contrasts with a low AI, precipitation may contrast with seasonally high temperatures, such as in drylands.

Human factors

The presence and intensity of human activities drives forest changes (IPCC, 2022). To account for these factors, we included annual 1-km-resolution data on night-time lights (NTL; Li et al., 2020). Additionally, we accounted for the fact that forest-management regimes and related human drivers often vary between countries (Herrera et al., 2019) by assigning unique country identifiers to each pixel (based on the Global Administrative boundary dataset; GADM, UCB, 2012). This served as a fixed spatial effect in our model.

Model quality assessment

We tested our model using spatial block cross-validation (Roberts et al., 2017). We iterated through each level-1 administrative unit in the GADM dataset (i.e., district- or state-level), withholding the corresponding samples to validate a model trained with the remainder. We then recorded the predictions for the withheld sample locations to subsequently evaluate model performances. Through this process, we evaluated our ability to predict tree-canopy cover in pixels beyond an area occupied by reference data. We chose level-1 administrative units instead of countries for the block validation, because we included a country-level fixed effect, and decision-tree algorithms cannot predict out-of-sample.

We compared the pooled predictions for all administrative units against the respective reference values to derive the coefficient of determination (r^2), the Root Mean Square Error (RMSE), and the F1-score (Taha and Hanbury, 2015) The r^2 and the RMSE measure the quality of fit. The former shows how well we capture spatial gradients in the reference data, whereas the latter quantifies the magnitude of prediction errors. In turn, the F1-score evaluates the predicted presences and absences of tree-canopy cover, controlling for high commission errors hidden by low prediction errors.

We mapped tree-canopy cover by exploring temporal path-dependencies in tree cover change. This enabled us to reconstruct historical changes since 1992, although the earliest instance of our reference data on tree-canopy cover is available for the year 2000. To test our model's reconstruction ability, we evaluated our quality metrics separately for pixels that, according to the GFC dataset, experienced no (0 ha), small (>0 - <1 ha), medium (1 - <4 ha), or large (≥ 4 ha) losses. We focused on losses because gains as depicted in the GFC dataset are estimated as a mask, and provided solely for the 2000-2012 period. Despite this, it is important to reiterate that we do not predict changes in tree-canopy cover, but rather year-specific percentages, changes in which are mostly driven by losses.

Additionally, we tested our model's ability to predict tree-canopy cover with different numbers of years separating the prediction year (t) and the future reference year (T). We anticipated that larger temporal gaps would be easier to predict given our model exploits long-term change processes. To this end, we tested the performance of our model for each year for the 2000-2007 period (8 years). This emulates backward-predictions for the 1990s, when high-resolution reference data on forest dynamics is missing. Temporal gaps between mapping and reference years vary (from 1 year for 1999 predictions with a 2000 reference to 8 years for 1992 predictions with a 2000 reference).

We ran our quality assessments for each region and continent distinguished by the United Nations Food and Agriculture Organisation (FAO) when compiling Forest Resource Assessments (FRA's), as to inform on the potential value of our data product in supporting these assessments.

Comparison with national statistics

Forest Resource Assessments (FRAs) provide the most authoritative national-scale information on forest extents across multiple decades. Because our data on tree-canopy cover dynamics may be viewed as complementary to the assessment of forest extents, we compared them to FRAs to assess the plausibility of the mapped national, regional, and global patterns.

Tree-canopy cover is conceptually distinct from forest cover as reported in FRAs, primarily because the latter not only accounts for areas immediately covered by canopies, but also for open areas in between trees. In addition, FRAs limit forest accountancy to tree stands ≥ 5m tall that cover ≥ 0.5-1.0 ha with a tree-canopy cover of ≥ 10%, and excludes tree-covered lands under non-forest uses (e.g., agricultural tree plantations, corresponding to ~2.3% of the global tree cover in 2015; FAO, 2016). In comparison, we based our model on data that aims to map tree occurrences with a height of ≥ 5m, but at a higher spatial resolution (0.09 ha). This is likely to make our modelled outputs more sensitive to the presence of trees compared to FRAs.

These conceptual differences prevent a direct comparison of mapped areas. Instead, we correlated national forest areas from FRAs with those estimated from the combined area of pixels for which we mapped some tree-canopy cover (describe tree covered landscapes, hereafter "treescapes"). The comparison between these variables follows the premise that, despite conceptual differences, treescape and forest extents should show similar cross-country variations.

We made comparisons against national forest-area statistics available for 1990, 2000, 2010, 2015, and 2020, and estimated their correlation (r^2) against national treescapes calculated from our product for the nearest mapping years (i.e., 1992, 2000, 2010, 2015, and 2018). In addition, we compared the FRA of 2000 to treescapes derived from GFC's data. This assessment informed on our ability to generate regional predictions of a comparable quality to the GFC, which was derived with optical remote sensing data, and is therefore informed by visual evidence of tree occurrences.

We correlated national treescape areas with national accountings of forest areas using weighted least-squares regression. The weights are country-specific and based on the reliability of FRA data based on national remote-sensing and forest-inventory capabilities (Nesha et al., 2021). Although monitoring capabilities are graded on individual FRA years, we used a static weight because grades were only available since 2005. For each country and FRA year, we calculated the minimum value across FRA years, preventing countries with evolving capabilities to bias earlier FRA comparisons.

We used our correlation analysis across multiple FRA years to evaluate the stability of our predictions. Yet, not every country contributed to FRAs in every assessment year, and the data for some countries may be unreliable due to poor monitoring capabilities in some years. Therefore, we excluded two countries without data in every target year, 93 with weights of 0 (i.e., very poor-quality reports), and eleven where the GFC reported no forest cover despite contrary indications in the FRAs due to a lack of usable Landsat acquisitions. Overall, we included 132 out of 238 territories (28/48 in Asia, 33/56 in the Americas, 40/59 in Africa, 23/50 in Europe, 8/24 in Oceania).

From the remaining data pool, treescapes are unequally distributed across countries. In particular, countries with advanced monitoring capabilities and large forest extents (e.g., Brazil) received higher weights, and thus had a stronger influence over the direction of the regression line. This results in relatively low residuals that inflate correlations. To tackle this issue, we log-transformed both forest-areas and treescape extents prior to the correlation analysis to give a 'bigger voice' to countries with relatively small forest extents.

Change analysis

Tree-canopy cover influences multiple goals and targets of the 2030 Agenda for Sustainable Development (Estoque et al., 2021). Consequently, knowledge on historical patterns and directions of change is essential to refine post-2020 political action. Following this premise, we explored our data product to provide insights into long-term patterns of change in tree-canopy cover.

To achieve this, we first applied the Mann-Kendall test to the 1992-2018 time-series of each pixel to categorise significant negative and positive slopes as "losses" or "gains", respectively. We defined a trend as "significant" if the p-value reported by the Mann-Kendall test was ≤ 0.005, following recent recommendations for such assessments (Ioannidis, 2018). Then, for each trend category, we derived statistics within each combination of continent and forested biomes distinguished by the FAO (i.e., 'boreal', 'temperate', 'tropical dry', and 'tropical moist').

For each change category, biome, and continent, (**Fig. 4a-d**), we summed the area of the corresponding pixels to inform on the extent of the affected area (hereafter referred to as 'treescape extent', **Fig. 4b-c**). Then, for the pixels accounted for in each change category, we calculated the difference in tree-canopy cover between the first and last years of our time-series, informing on the change in the openness of the canopies (**Fig. 4e-f**). Whereas the first metric informs on the spatial dispersal of change dynamics, the second informs on the magnitude of those changes.

RESULTS

Quality assessment

Focusing on stable pixels (i.e., those not experiencing losses in tree-canopy cover), performances were higher across temporal gap sizes between the reference and target years. Within this group, r^2, RMSE, and F1-score values were, respectively, 0.99 (< ±0.01), 0.06 ha (±0.01) and 0.98 (±0.05) for gap sizes of 8 years, and 0.98 (< ±0.01), 0.16 (±0.03), and 0.95 (< ±0.01) for gap sizes of 1 year.

For changing pixels, correlations between predicted and reference values varied between 0.83 (±0.01) for temporal gaps of 1 year, and 0.93 (< ±0.01) for gaps of 8 years. When disaggregating these values per change-size class, we recorded a correlation of 0.98 (±0.01) for small to mid-sized changes with both 1 and 8 gap years, which for large changes dropped to 0.89 (±0.01) for a gap size of 8 years, and 0.73 (±0.01) for a gap size of 1 year. Similarly, RMSE values across small and mid-sized changes were lower for gap sizes of 8 years (0.40 ha, ±0.01) compared to gap sizes of 1 year (0.59, ±0.01), and differences increased for large changes (3.26 ha [±0.31] for 1 year, and 1.32 ha [±0.15] for 8 years). In contrast, F1-scores were persistent across gap sizes and change magnitudes (0.99 [±0.01]), suggesting our ability to correctly perceive presences and absences of tree cover.

When comparing our predicted treescape extents against national forest extents reported by FRAs, we recorded an r^2 of 0.94 in every assessment year (±0.00, **Fig. 3a-b**, see **Fig. 4 of SI** for plotted uncertainties). Moreover, the GTCCC-FRA correlation for the year 2000 was as strong as the GFC-FRA correlation, both globally (**Fig. 3c**) and regionally (**Table 3 of SI**).

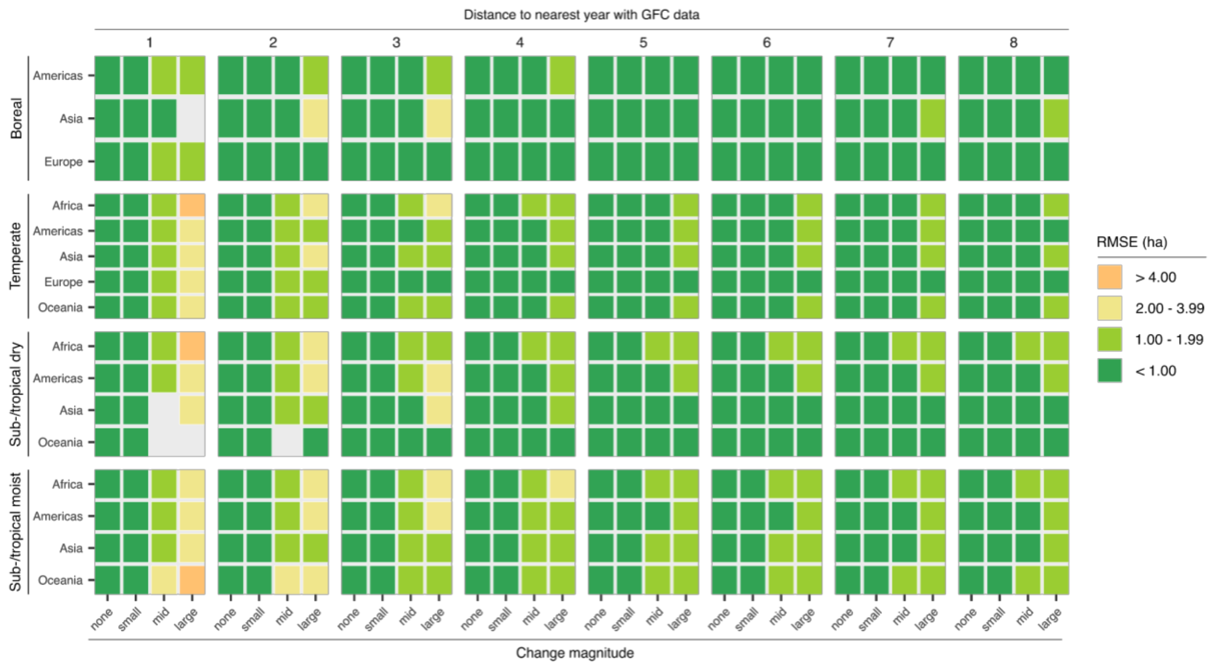

Figure 2 – Model quality. RMSE of predicted tree-canopy cover for different time intervals between the focal mapping year and the nearest year with reference data (shown in the header of each block), and for different continents, biomes, and tree-canopy cover change sizes. The uncertainties surrounding the values in this plot are displayed by **Fig. 3 of SI.**

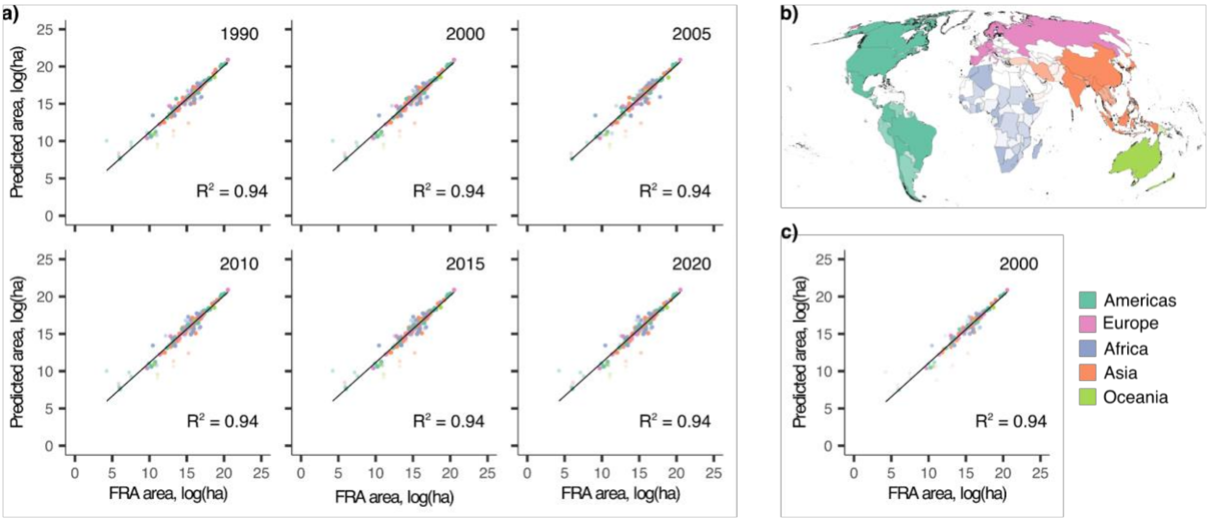

Figure 3 – Alignment of global patterns of treescape extents with FRA data on forest extents. **a**) Cross-country correlations of national extents of treescapes derived from the GTCCC with forest extents reported in FRA statistics for each reporting year (see **Fig. 4 of SI** for plots on upper/lower confidence bounds). The colour of points distinguishes geographical regions (**b**); countries shown in white were excluded from this comparison due to filtering. Correlations were weighted by the quality of national reporting capabilities, which are indicated in **b)** by varying levels of transparency. Solid colours indicate high quality data. **c**) As in **a)**, but comparing FRA data for 2000 to the GFC.

Changes in treescape extents

We estimated global net losses in treescape extents of 8.8 million ha (Mha, ±0.4) based on pixels with significant long-term trends (**Fig. 4a-c**, **Table 1**). The largest net losses were visible across the tropics (-11.5 Mha, ±0.6), 60.0% and 40.0% of which occurred in the tropical moist and tropical dry biomes, respectively (**Table 1**). Although the tropical moist biome experienced larger global losses in treescape extents, tropical dry losses were larger in Africa (-1,0 Mha [±0.0] vs -0.6 Mha [±0.0]).

At higher latitudes, treescape gains within the temperate biome become more common than losses, minor negative balances in North America (-0.4 Mha, ±0.0). Globally, temperate treescapes increase by 3.6 Mha (±0.1), 90.5% of which occurred in Europe (3.2 Mha, ±0.0). Gains in Europe correspond to +1.2% relative to 1992 (±0.0), second only to Australia (+2.3%, ±0.0).

Despite these gains, we again observed net losses in treescape extents at higher latitudes. The boreal biome experienced global net losses (-0.9 Mha, ±0.5), with nearly twice as much area lost in Asia as was gained in Europe (-1.0 Mha [±0.3] vs. +0.6 Mha [±0.0]).

Changes in tree-canopy cover

Whereas our analysis of changes in treescape extents revealed regional contrasts, we found systematic losses in tree-canopy cover across all biomes and continents (-175.1 Mha [±1.0], **Fig. 4d-f**, **Table 1**). The bulk of these losses (58.7%) occurred in the tropical moist biome (-102.9 Mha, ±2.5), and was 27 times greater than the simultaneous loss in the extent of treescapes.

Losses within the tropical moist biome predominantly occurred in South America (43.7% of net losses, -45.0 Mha [±0.9]). By comparison, the tree-canopy cover over the tropical dry biome decreased by -11.6 Mha (±0.0), nearly 9 times smaller than the losses in the tropical moist biome. However, this change is larger if viewed as a net percentage loss relative to the 1992 baseline (-7.5% [±0.0] vs -10.4% [±0.1] for tropical moist and tropical dry, respectively).

In the temperate biome, treescape and tree-canopy cover dynamics showed contrasting directions of change. The net losses in tree-canopy cover (-33.0 Mha, ±1.0) were nine times larger than the areal net gains in treescape extents (corresponding to a loss of -6.3% [±1.0] relative to the 1992 baseline).

Even Europe's gains in temperate treescape extents were superseded nearly 1.7-fold by losses in tree-canopy cover (**Table 1**). In fact, net losses consistently dwarfed absolute net changes in treescape extents in all biomes and continents, typically by an order of magnitude or more (e.g., corresponding to a 93 times larger area in the tropical moist biome in Asia).

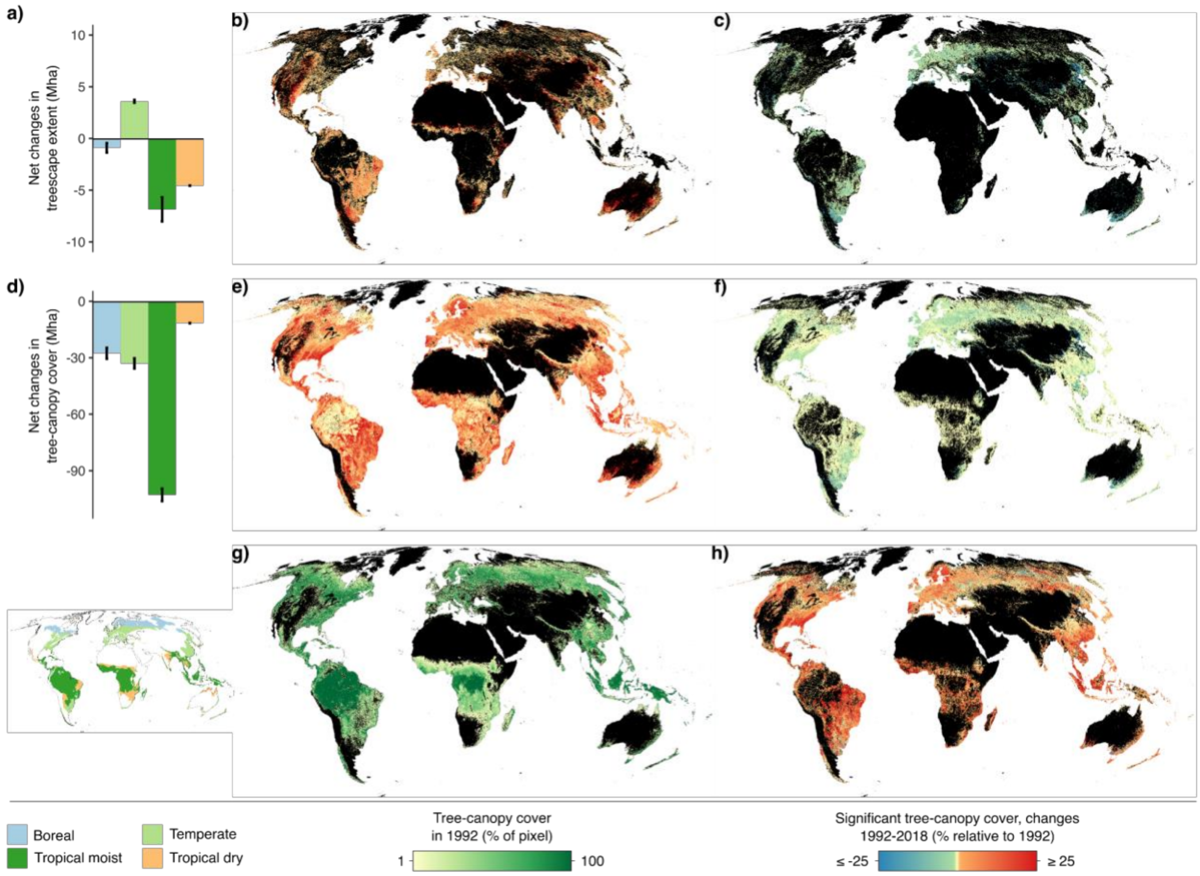

Figure 4 – Global changes in tree-canopy cover and treescape extents. Global net changes of treescape extents (**a**) and tree-canopy cover (**d**) for different biomes over the 1992-2018 period, based on statistically significant trends (gains or losses) detected at a 300-m resolution (biomes indicated by bar colours, and mapped below), and aggregated for mapping to a 10-km resolution. **b**/**c**) Global percent losses (**b**) and gains (**c**) in treescape extents, relative to the 1992 baseline (shown in **g**). **e**/**f**) Global percent losses (**e**) and gains (**f**) in tree-canopy cover (same baseline). **h)** Net changes (i.e., losses or gains) in tree-canopy cover evaluated at the 10-km mapping resolution, highlighting a global dominance of net losses.

Table 1 – Global change in treescape extents and tree-canopy cover. Net 1992-2018 changes in treescape extents and tree-canopy across biomes and regions. Expressed in millions of ha (Mha) and as percentages (%) of the 1992 baseline.

Biome	*Continent*	***Δ Treescape extent (1992-2018)***		***Δ Tree-canopy cover (1992-2018)***	
		Δ (Mha)	Δ (% of 1992 extent)	Δ (Mha)	Δ (% of 1992 cover)
All	**World**	**-8.8 (±0.4)**	**-8.8 (±0.4)**	**-8.8 (±0.4)**	**-7.3 (±0.0)**
	Africa	-1.6 (±0.0)	-0.2 (±0.0)	-29.1 (±0.4)	-6.8 (±0.0)
	Asia	-1.6 (±0.4)	-0.2 (±0.0)	-43.4 (±1.4)	-8.1 (±0.0)
	Australia	0.5 (±0.0)	0.9 (±0.0)	-1.1 (±0.0)	-6.9 (±0.0)
	Europe	3.8 (±0.1)	0.9 (±0.0)	-15.2 (±0.4)	-7.2 (±0.0)
	North America	-0.9 (±0.3)	-0.2 (±0.1)	-31.6 (±0.8)	-10.4 (±0.0)
	Oceania	< 0.1	0.1 (±0.0)	-0.7 (±0.0)	-4.2 (±0.0)

	South America	-8.9 (±1.0)	-0.8 (±0.1)	-54.0 (±1.1)	-7.2 (±0.0)
Boreal	**World**	**-0.9 (±0.5)**	**-0.1 (±0.1)**	**-27.6 (±0.7)**	**-7.5 (±0.0)**
	Asia	-1.0 (±0.3)	-0.3 (±0.1)	-10.6 (±0.2)	-6.8 (±0.1)
	Europe	0.6 (±0.0)	0.3 (±0.0)	-7.3 (±0.2)	-7.2 (±0.0)
	North America	-0.5 (±0.1)	-0.3 (±0.1)	-9.7 (±0.2)	-8.9 (±0.0)
Temperate	**World**	**3.6 (±0.1)**	**0.4 (±0.0)**	**-33.0 (±1.0)**	**-8.1 (±0.0)**
	Africa	0.0 (±0.0)	0.2 (±0.0)	-0.4 (±0.0)	-10.3 (±0.1)
	Asia	0.1 (±0.0)	0.0 (±0.0)	-6.1 (±0.1)	-5.5 (±0.0)
	Australia	0.5 (±0.0)	2.3 (±0.0)	-1.0 (±0.0)	-9.9 (±0.1)
	Europe	3.2 (±0.0)	1.2 (±0.0)	-7.9 (±0.2)	-7.2 (±0.0)
	North America	-0.4 (±0.1)	-0.2 (±0.0)	-15.1 (±0.5)	-11.0 (±0.0)
	Oceania	< 0.1	0.2 (±0.1)	-0.3 (±0.0)	-5.0 (±0.0)
	South America	0.1 (±0.0)	0.1 (±0.0)	-2.2 (±0.1)	-7.9 (±0.1)
Tropical dry	**World**	**-4.6 (±0.0)**	**-1.0 (±0.0)**	**-11.6 (±0.0)**	**-10.4 (±0.1)**
	Africa	-1.0 (±0.0)	-0.4 (±0.0)	-2.8 (±0.0)	-6.7 (±0.0)
	Asia	-0.4 (±0.0)	-0.7 (±0.0)	-1.5 (±0.0)	-10.4 (±0.1)
	Australia	- < 0.1	- < 0.1	- < 0.1	-1.0 (±0.0)
	North America	-0.1 (±0.0)	-0.5 (±0.1)	-0.5 (±0.0)	-6.3 (±0.0)
	South America	-3.0 (±0.0)	-2.6 (±0.0)	-6.8 (±0.0)	-15.6 (±0.1)
Tropical moist	**World**	**-6.9 (±1.2)**	**-0.3 (±0.1)**	**-102.9 (±2.5)**	**-7.5 (±0.0)**
	Africa	-0.6 (±0.0)	-0.1 (±0.0)	-26.0 (±0.5)	-6.8 (±0.0)
	Asia	-0.3 (±0.0)	-0.1 (±0.0)	-25.2 (±1.0)	-9.9 (±0.0)
	Australia	< 0.1	0.2 (±0.0)	- < 0.1	-2.6 (±0.0)
	North America	0.1 (±0.1)	0.1 (±0.1)	-6.2 (±0.1)	-13.1 (±0.1)
	Oceania	- < 0.1	- < 0.1	-0.4 (±0.0)	-3.6 (±0.0)
	South America	-6.1 (±1.0)	-0.7 (±0.1)	-45.0 (±0.9)	-6.7 (±0.0)

DISCUSSION

We integrated remotely sensed information with complementary strengths to reconstruct global tree-canopy cover dynamics over nearly three decades. This offers new opportunities for assessing long-term changes in forests and other wooded ecosystems, analysing their impacts on biodiversity, training climate models, prioritising sites for ecosystem restoration, and various other applications supporting the 2030 Agenda for Sustainable Development. In turn, our analyses of the GTCCC offer new insights into the magnitude, direction, timing, and speed of global and regional tree-canopy cover changes, adding important nuance to previous forest change assessments.

Our analyses indicate that, since the early 1990s, wooded landscapes experienced systematic losses in tree-canopy cover at global, continental, and biome scales. These canopy-cover losses substantially exceed concurrent losses or gains of treescape extents. These results are in line with contrasts between trends in deforestation and forest disturbance reported from various regions (Aryal et al., 2021; Chen et al., 2021; Qin et al., 2021; Shapiro et al., 2021), and imply that common practices of estimating carbon-budget trends based on categorical land cover (e.g., Alkama and Cescatti, 2016; Baccini et al., 2017; Friedlingstein et al., 2022) may underestimate carbon losses.

Even in Europe, where forests are reportedly larger today than in the 20th century (Estoque et al., 2022), net gains in temperate and boreal treescape extents are dwarfed by concurrent losses in tree-canopy cover. Surprisingly, canopy-cover losses are noticeable across Eastern Europe (**Fig. 4e**), despite this being the European subregion with the largest treescape gains (**Fig. 4c**). These results are consistent with previous reports of increasing patch sizes and frequencies of forest disturbances (Senf and Seidl, 2021), which have been linked to increases in wood harvests, and natural disturbances such as insects, windthrow and fires (McDowell et al., 2020; Seidl et al., 2014; Senf et al., 2018).

We note that our data neither indicate specific causes nor mechanisms of canopy-cover losses, which can affect carbon retention and other forest functions (Luyssaert et al., 2008; Thom and Seidl, 2016). Irrespective, the relative magnitude of tree-canopy cover losses relative to those in treescapes indicates that ignoring the former likely misses changes in those functions. Our results corroborate recent calls for better accountings of forest disturbances in European environmental policies (Maes et al., 2023), which currently aim solely for net increases in forest extents under the Green Deal, and which do not explicitly promote non-urban canopy cover gains (European Commission, 2022).

Similarly, our results indicate that even in countries with high national forest-monitoring capacities, the use of categorical data can grossly misrepresent structural changes in forest. For example, authoritative categorical data on canopy cover developed for Australia (Lucas et al., 2019) reveals net gains in temperate rainforests of +2.8% (-6.3%/+9.0%) between 1996 and 2016, whereas the Forest Practice Authority of Tasmania reported a loss of -3.7% during the same period (FPA, 2017). Our data integration framework enabled the detection of similar losses (-3.2%, ±0.2). Literature relates these changes to growing human pressures in the form of logging and mining, and to the increasing risk of fires driven by climate change (Mackey et al., 2017). The latter, in particular, lead to rainforest losses in recent years, such as seen over the Tarkine region of Tasmania (**Fig. 5b-c**).

Especially in tropical moist forest regions, where the historical Landsat archive has extensive temporal gaps during the 1990s (Wulder et al., 2016), integrating complementary data sources provided novel perceptions of the onset of major forest disturbances. For example, Côte d'Ivoire's Marahoué National Park (**Fig. 5e**) experienced extensive human settlement and the near-complete conversion of its forest area into cocoa plantations, both of which contributed to steep population declines in Western chimpanzees and other threatened primate species (Bitty et al., 2015; Campbell et al., 2008; Kühl et al., 2017). Landsat-based categorical time-series (Vancutsem et al., 2021) depict stable forest cover throughout the 1990s, with extensive forest degradation and deforestation thereafter. In contrast, by integrating data available during the 1990s only at coarse resolutions, we detected finer-resolution changes during this decade that make up for ~1/3 of 1992-2018 tree-canopy-cover losses (**Fig. 5f**, -8,085 ha vs. -17,006 ha), consistent with regional reports (**Fig. 5f**, -8,085 ha vs. -17,006 ha), consistent with regional reports (Hauhouot, 1992; Kouakou et al., 2018).

As we learned about these changes, we noted contrasts between tropical moist and dry biomes. In line with national statistics, we found the largest tree-canopy cover losses over the tropical moist biome (FAO, 2020) that threaten millions of species (Pillay et al., 2022) and historical carbon sinks (Achard et al., 2014). These risks earned the tropical moist biome disproportionate attention in literature compared to the tropical dry biome (Schröder et al., 2021). However, we found that the tropical dry biome experienced larger percent losses to its naturally sparser tree-canopy cover. This result supports calls for attention towards tropical dry woodlands (Schröder et al., 2021), on which millions of people depend as a source of fuelwood (Blackie et al., 2014).

Within tropical dry forests, change patterns and speeds are often heterogeneous (Buchadas et al., 2022). For example, in the surroundings of the Cangandala National Park in Angola (**Fig. 5h-i,** World Bank, 2019), the emergence of fast-paced changes associated with industrial farming (such as near the town of Cangandala, **Fig. 5i**) contrasts with slow-paced changes plausibly explained by household consumption of woodlands for fuelwood that is typical in the region (Michael Mills, 2017).

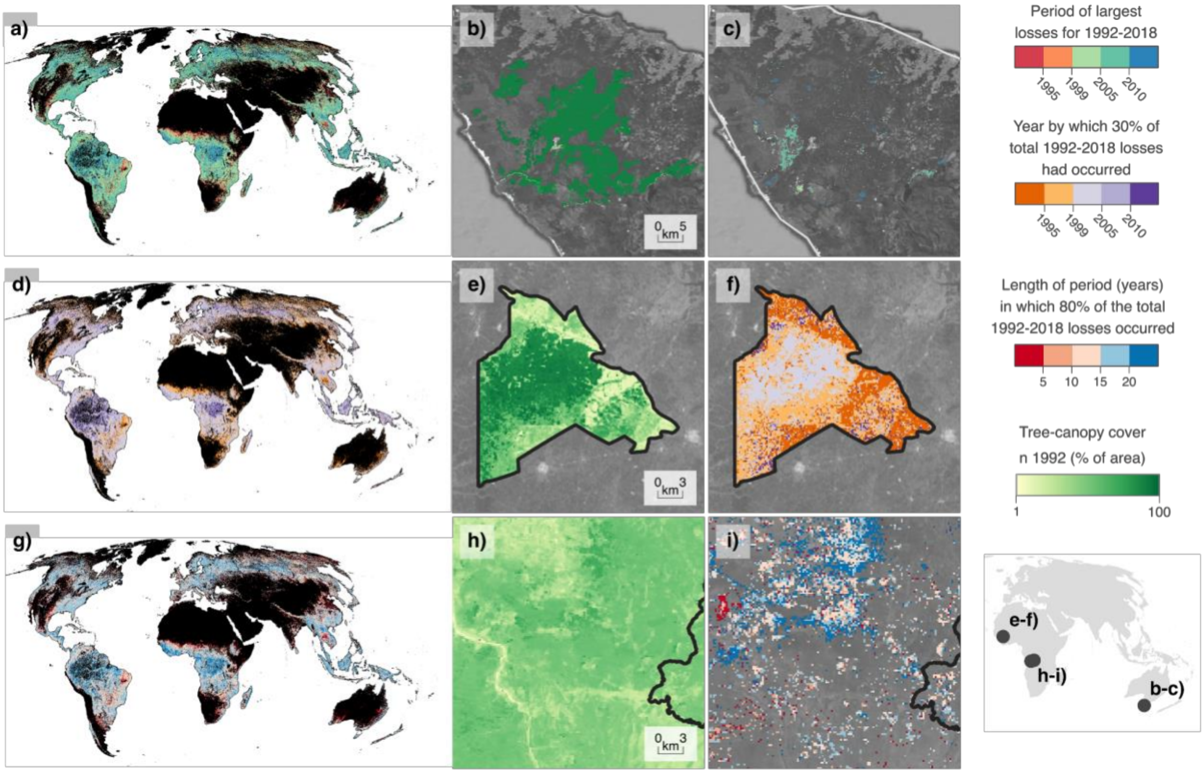

Figure 5. Temporal dynamics in tree-canopy cover. Multi-temporal change metrics describing the timing and speed of tree-canopy cover changes over the 1992-2018 period, computed based on 300-m pixels experiencing significant losses (slope < 0; p-value < 0.0005). Panels **a**/**d**/**g** show global patterns of change dynamics (means per 3-km pixel); **c**/**f**/**i** show local examples, with **b**/**e**/**h** showing the initial (1992) tree-canopy cover for reference. **a**/**c)** Period experiencing the largest losses in tree-canopy cover. **b)** The Tarkine in north-eastern Tasmania is Australia's largest old-growth temperate rainforest, known for its high integrity (note the continuous dense canopy cover in 1992; rainforest extent delineated by authoritative data (DPIPWE, 2020)). **c**) Forest disturbances within the Tarkine, mainly after 2005. **d**/**f)** Year by which 30% of the total 1992-2018 net tree-canopy cover losses had occurred. **e**/**f)** Cote d'Ivoire's Marahoué National Park was in 1992 still covered by tropical moist forest and savanna, which by the late 2000s had been nearly completely converted. The GTCCC perceives losses within Cote Ìvoire's Marahoué National Park already in the 1990s (**e,** orange tones), with continuous losses into densely tree-covered portions of the park in the 2000s. **g)** Speed of tree-canopy losses, expressed as the length of the shortest possible contiguous period (in years) within which 80% of the total 1992-2018 net losses occurred. Outside of Angola's Cangandala National Park (**h-i,** outlined in black), faster miombo losses (i.e., <5 years, in bright red) coincide with the emergence of industrial farming, which contrasts with slow changes (i.e., > 20 years, shown in blue) likely associated with small-scale farming and charcoal-collection.

Opportunities for more reliable monitoring and & scenario-based assessments

We found a strong correlation between FRAs and our data when equating the quality of national reporting capabilities (Nesha et al., 2021). This suggests our data is aligned with national views on the extent of forest resources. While tree-canopy cover is not directly comparable to 'forest' as a land-use class as referred to in FRAs, the GTCCC can be combined with ancillary data to support more reliable assessments of the drivers of long-term losses and gains in forest extents. Moreso, it may support complementary assessments of the conditions of forests and other wooded ecosystems (e.g., disturbance-succession dynamics due to climate change, Lantz et al., 2022; or forest-management regimes, Ankomah et al., 2019) , which is highly relevant for multiple goals and targets of the 2030 Agenda for Sustainable Development (Estoque et al., 2021).

Note, however, that we reported treescape losses much smaller than those for forest cover (e.g., -0.45% vs. -17% in Vancutsem et al., 2020 for the tropical moist region). This is to be expected due to differences in mapping concepts (i.e., irrespective of additional influences of different mapping resolutions and possible data errors). Whereas categorical forest-cover data will map losses as soon as tree-cover is no longer perceived as dominant in the respective pixels, treescape extents will not show losses for as long as the underlying continuous tree-canopy cover layers perceive any trees. Correspondingly, perceived canopy-cover losses may reflect diverse processes, including woodland fragmentation or reduction of patch sizes (e.g., moving deforestation frontiers), disturbances (e.g., landslides, windthrow), canopy thinning via selective harvesting or natural dying of individual trees, removal of small tree stands from largely treeless landscapes, as well as transitions from higher- to lower-density wooded ecosystems (e.g., forest to savanna). The GTCCC may thus support assessments of changes in extent or condition of different wooded ecosystem types, particularly if combined with other information distinguishing these processes.

In particular, studies of wooded ecosystem disturbances or fragmentation and related biological processes should consider whether expected canopy gaps in their study areas will be large enough to cause detectable breaks in canopy-cover gradients among neighbouring pixels. The GTCCC's pixel size (~9 ha at the equator) is at the lower ends of reported ranges of average deforestation patch sizes in Amazonia (10.6–24.7 ha; Trancoso, 2021), and average disturbance-patch sizes in moderately disturbed forest landscapes sampled across the temperate-forest biome (6.96–41.47 ha; Sommerfeld et al., 2018). However, disturbance patches are much smaller in low-disturbance temperate-forest landscapes (0.46–0.85 ha; Sommerfeld et al., 2018), and generally in European forests (mean size of 1.09 ha; Senf and Seidl, 2021). Similarly, the GTCCC data may not support meaningful assessments of habitat fragmentation for species whose maximum dispersal abilities fall well below the ~300-m pixel size (e.g., many species with body sizes smaller than ~150g/~15 cm; Stevens et al., 2014).

Besides applications in monitoring, the GTCCC can support climate modelling. Tree-canopy cover is an essential climate variable (WMO, 2022), and plays an important role in global and regional climate modelling (Gou et al., 2019). These data can more accurately inform translations of land-cover classes into fractional coverages of plant functional types, which is critical to link climate and ecosystem models (Bonan et al., 2002; Lawrence and Chase, 2007).

The derived climate models can then be used to infer climate normals against which to measure climate change (WMO, 2017), for which 30 years of observations are recommended to detect anomalies (WMO, 2017). For such long-time scales, however, long-term and continuous canopy-cover information had thus far only been available at coarse spatial resolutions (i.e., 5-km; Song et al., 2018) that may not meet spatial-resolution requirements of climate models (e.g., ≤1-km for carbon modelling; Zhao et al., 2010). With 27 years at 300-m resolution, the GTCCC thus offers improved support for climate change assessments.

Combining strengths to overcome individual weaknesses

We built our data product with a novel modelling framework that explores complementary strengths of multiple existing products. For example, the use of data on land-cover allowed our model to learn how class distinctions relate to both averages and spreads of associated tree-canopy-cover values. This enabled our model to predict more plausible spatial patterns of flat vs. steep tree-canopy gradients, benefitting from a categorical product's ability to perceive transitions in tree-canopy cover dominance. In addition, by using data on coarse-scale (but temporally complete) vegetation changes compared to a future, reference year, and by relating those changes to the spatial distribution of high-resolution tree-canopy cover in that year, our model learned from the outcomes of longer-term change processes, which are co-informed by change drivers in the mapping years (i.e., climate, topography, human activity).

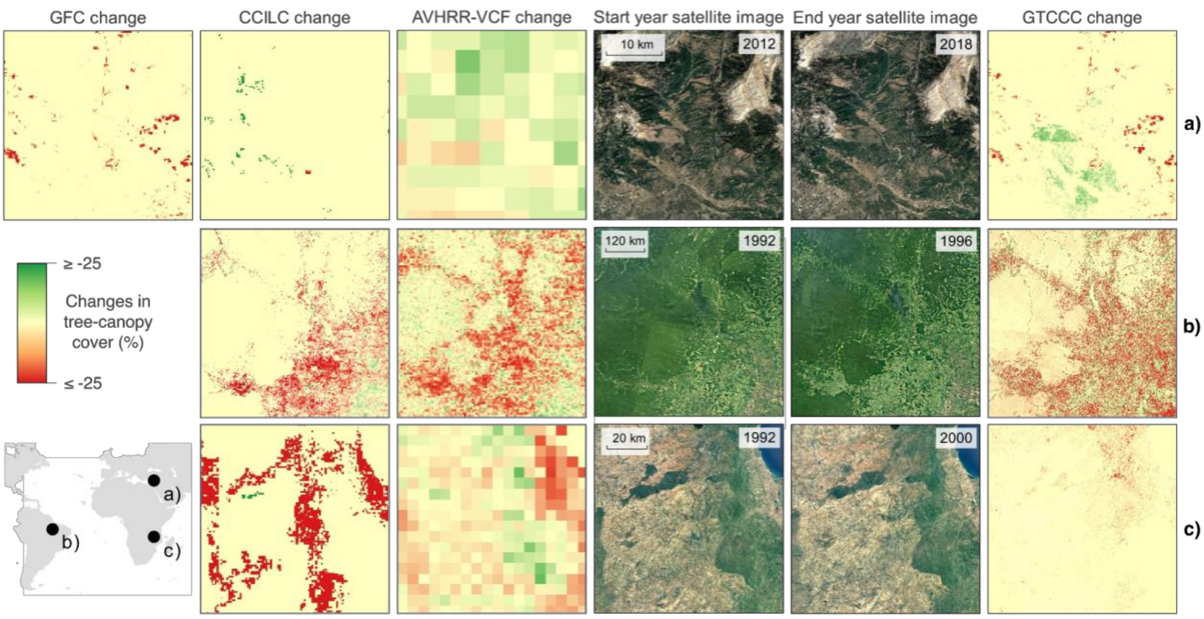

Figure 6 – Mapping new tree-canopy cover changes. Each row of figures (labelled as **a**, **b** and **c**) shows a regional example (locations in inset map) of tree-canopy cover losses and gains as perceived by our new product (GTCCC; right) and by three of its inputs (GFC, CCILC, AVHRR-VCFI; left to centre) during different time periods. Those periods' start/end years are indicated in columns 4/5, which show Landsat-based true-colour images for the respective years for visual confirmation of true change patterns. The three examples show different ways in which the GTCCC improves change depictions compared to those of each input product taken individually. **a**) In southern Turkey, visible post-fire forest succession during the mid-2010s is realistically captured as tree-canopy-cover gains in the GTCCC. By contrast, the CCILC only partially captures these but instead maps large patches of gains elsewhere that are unsupported by visual inspection, as does the coarser-resolution AVHRR-VCF, whereas the GFC by design only depicts losses. **b**) Regional patterns of tree-canopy-cover losses across a north-eastern Amazonian deforestation frontier during the 1990s are broadly captured by both the CCILC and AVHRR-VCF products. Yet, the new GTCCC product shows these patterns more completely than the CCILC and more refined than the AVHRR-VCF. **c**) In a part of southern Malawi, the CCILC depicts extensive losses between 1992 and 2000, while the AVHRR-VCF shows extensive mixtures of losses and gains. By contrast, the GTCCC depicts only minor losses and gains, more consistent with Landsat true-colour images showing that tree-canopy cover has remained largely unchanged during that period. The GFC is not included in b/c, as it only maps post-2000 losses.

Through this data integration process, our model was able to generate temporal patterns with fewer outliers and back-and-forth changes compared to our input data (**Fig. 5 of SI**), as well as more plausible regional patterns of tree-canopy cover changes compared to those perceived by individual inputs (**Fig. 6**). For example, the GTCCC better captures tree-canopy cover gains than either of the two input products that are sensitive to tree-canopy cover (i.e., AVHRR-VCF, CCILC; note that the GFC does not attempt to map gains past 2012; **Fig. 6a**). Simultaneously, the GTCCC could capture more complete patterns of gains and losses during the 1990s than the CCILC and AVHRR-VCF products (**Fig. 6b**). The model-based data-integration process also allowed correcting inaccuracies in individual products. For example, the CCILC product mapped losses of >30% (Radwan et al., 2021) during the 1990s in areas of southern Malawi that, according to visual evidence, had already been largely treeless by the beginning of that period (**Fig. 6c**). In turn, the GTCCC mapped negligible losses (-0.04% [±0.03]).

Data quality and caveats

The quality assessment of the GTCC yielded a high r^2 (≥0.95), and a relatively low RMSE (< 1 ha). Yet, we found that the RMSE decreased with increasing temporal gap sizes (between the mapping year and the nearest year with reference data on tree-canopy cover), and with increasing tree-canopy covers to be reconstructed. In addition, our modelling framework had difficulties reconstructing mid-sized and large changes (2-4 ha and ≥4 ha, respectively) over periods of 1-3 years.

By contrast, our data performed consistently across continents and biomes when predicting small changes, and when predicting mid-sized and larger changes over ≥4 years. This indicates that the GTCCC is most suitable for studying mid- to long-term change dynamics across 4-year epochs, and is not generally suitable to analyse the timing of fine-scale changes.

Literature shows that most changes in tree-covered landscapes are path-dependent, multi-year processes (Taubert et al., 2018), whereas changes that are simultaneously extensive and fast are rare (Montibeller et al., 2020).However, like most global products, the GTCC is designed for broad-scale applications where specific, pixel-level errors may be expected to average out. Any smaller-scale studies that depend on highly accurate pixel-level patterns should use the GTCCC cautiously and ideally after assessing its specific fitness-for-purpose (e.g., via a local validation).

We validated our model's ability to predict tree-canopy cover as perceived by the GFC, a state-of-the-art product which we used as a source of samples and whose quality we aimed at replicating. In addition, we tested the plausibility of our predicted global treescape patterns via comparison against the most authoritative global information on the distribution of forest resources. Yet, it was not feasible to validate tree-canopy cover values independently due to a lack of globally representative and independent validation data at relevant spatial resolutions (i.e., 300-m or coarser).

We caution users that although GFC's tree-canopy cover data was developed using very-high-resolution imagery, and tree-cover losses were carefully validated against independent data (Hansen et al., 2013), our random-forest model borrows its strengths along with its weaknesses. In particular, our data cannot correct cases where the GFCCC (near-)completely misses tree-canopy cover over large regions, even if trees are better captured by other products (e.g., in north-eastern Somaliland, the GTCCC underestimates the extents of montane woodlands, whereas the CCILC depicts their presence more accurately). In addition, we are unable to predict tree-canopy cover over 0.54% of the land surface, a proportion composed mainly by pacific islands and desertic lands. This is related to the fact that Landsat imagery in these areas is scarce during the early 2000s (Remelgado et al., 2023), which prevented the GFC from predicting tree-canopy cover. Since changes are inferred from the 2000 baseline, changes thereafter are missing.

Going forward, such caveats could be addressed by integrating trusted regional products, both as source of samples and predictor data. Furthermore, forcing our machine-learning framework to consider prior theoretical understanding as exemplified in other disciplines (Seckler and Metzler, 2022; Wang et al., 2021) could help refine predictions by better acknowledging distinctions of biogeographical regions that, due to different plant adaptations, may result in specific relationships between tree-canopy cover and environmental predictors (Nicolson, 1996). Such future versions would ideally be able to rely on independent samples for validation (which are anyway a prerequisite for the existence of trustworthy regional products). Thus far, systematic efforts to derive standardised random validation samples from very-high-resolution imagery over broad spatial extents have been customised to serve modern satellite monitoring systems with higher spatial resolutions (e.g., up to a 100-m resolution; Tsendbazar et al., 2021). In the future, such systematic sampling designs could be extended to derive coarser-resolution reference data at least for recent years. Additionally, the opening of spy satellite archives holds promise for generating change-validation samples for many regions worldwide (e.g., as shown by Rizayeva et al., 2023). However, technical advances are still needed to reduce the manual effort required for generating analysis-ready images from these archives, a precondition for applying them at scale.

Concluding remarks

Model-based integration of existing remote-sensing products as showcased here cannot substitute continuous investments in higher-quality remote-sensing products based on intensive sampling and best-available algorithms for satellite-data interpretation. However, as hundreds of new remote-sensing products become available every year for different regions, scales, and application domains, there are additional opportunities in synthesising information in ways that enable additional insights or better meet the demands of certain user groups. We hope that our showcase may inspire further developments of modelling frameworks that effectively use the complementary strengths of different products to derive synthesis products that are more than the sum of their parts.

ACKNOWLEDGEMENTS

We developed this study with the High-Performance Computing (HPC) Cluster EVE, a joint effort by the Helmholtz Centre for Environmental Research (UFZ) and the German Centre for Integrative Biodiversity Research (iDiv) Halle-Jena-Leipzig. We were financed by the Volkswagen Foundation through CM's Freigeist Fellowship (A118199), with additional support by iDiv (FZT-118, DFG).

DATA AND CODE AVAILABILITY

The GTCCC and the code needed to produce it are available through Zenodo (https://doi.org/10.5281/zenodo.7901290). Its predictors, however, are provided through a separate Zenodo repository (https://doi.org/10.5281/zenodo.8217237).

AUTHOR CONTRIBUTIONS

RR and CM designed the study. RR developed the modelling framework with support from CM. RR developed the data products reported in this paper, including the underlying code. RR and CM interpreted the results. RR and CM wrote the paper.

CONFLICT OF INTEREST STATEMENT

We declare no conflict of interest.

REFERENCES

1. Achard, F., Beuchle, R., Mayaux, P., Stibig, H.-J., Bodart, C., Brink, A., Carboni, S., Desclée, B., Donnay, F., Eva, H.D., Lupi, A., Raši, R., Seliger, R., Simonetti, D., 2014. Determination of tropical deforestation rates and related carbon losses from 1990 to 2010. Glob. Change Biol. 20, 2540–2554. https://doi.org/10.1111/gcb.12605
2. Alkama, R., Cescatti, A., 2016. Biophysical climate impacts of recent changes in global forest cover. Science 351, 600–604. https://doi.org/10.1126/science.aac8083
3. Allen, C., Metternicht, G., Wiedmann, T., 2017. An Iterative Framework for National Scenario Modelling for the Sustainable Development Goals (SDGs). Sustain. Dev. 25, 372–385. https://doi.org/10.1002/sd.1662
4. Ankomah, F., Kyereh, B., Asante, W., Ansong, M., 2019. Patterns of forest cover change and their association with forest management regimes of forest reserves in the high forest zone of Ghana. J. Land Use Sci. 14, 242–257. https://doi.org/10.1080/1747423X.2019.1665116
5. Aryal, R.R., Wespestad, C., Kennedy, R., Dilger, J., Dyson, K., Bullock, E., Khanal, N., Kono, M., Poortinga, A., Saah, D., Tenneson, K., 2021. Lessons Learned While Implementing a Time-Series Approach to Forest Canopy Disturbance Detection in Nepal. Remote Sens. 13. https://doi.org/10.3390/rs13142666
6. Baccini, A., Walker, W., Carvalho, L., Farina, M., Sulla-Menashe, D., Houghton, R.A., 2017. Tropical forests are a net carbon source based on aboveground measurements of gain and loss. Science 358, 230–234. https://doi.org/10.1126/science.aam5962
7. Barrow, C.J., 1992. World atlas of desertification (United nations environment programme), edited by N. Middleton and D. S. G. Thomas. Edward Arnold, London, 1992. isbn 0 340 55512 2, £89.50 (hardback), ix + 69 pp. Land Degrad. Dev. 3, 249–249. https://doi.org/10.1002/ldr.3400030407
8. Baul, T.K., Chowdhury, A.I., Uddin, M.J., Hasan, M.K., Kilpeläinen, A., Nandi, R., Sultana, T., 2021. Forest carbon stocks under tree canopy densities in Sitapahar natural forest reserve in Chittagong Hill Tracts of Bangladesh. For. Ecol. Manag. 492, 119217. https://doi.org/10.1016/j.foreco.2021.119217
9. Bitty, E.A., Bi, S.G., Bene, J.-C.K., Kouassi, P.K., McGraw, W.S., 2015. Cocoa Farming and Primate Extirpation Inside Cote D'ivoire's Protected Areas. Trop. Conserv. Sci. 8, 95–113. https://doi.org/10.1177/194008291500800110
10. Blackie, R., Baldauf, C., Gautier, G., Gumbo, D., Kassa, H., Parthasarathy, N., Paumgarten, F., Sola, P., Pulla, S., Waeber, P., Sunderland, T., 2014. Tropical dry forests - The state of global knowledge and recommendation for future research. CIFOR, Bogor Barat, Indonesia.

11. Bonan, G.B., Levis, S., Kergoat, L., Oleson, K.W., 2002. Landscapes as patches of plant functional types: An integrating concept for climate and ecosystem models. Glob. Biogeochem. Cycles 16, 5-1-5–23. https://doi.org/10.1029/2000GB001360
12. Breiman, L., 2001. Random Forests. Mach. Learn. 45, 5–32. https://doi.org/10.1023/A:1010933404324
13. Buchadas, A., Baumann, M., Meyfroidt, P., Kuemmerle, T., 2022. Uncovering major types of deforestation frontiers across the world's tropical dry woodlands. Nat. Sustain. https://doi.org/10.1038/s41893-022-00886-9
14. Buchhorn, M., Lesiv, M., Tsendbazar, N.-E., Herold, M., Bertels, L., Smets, B., 2020. Copernicus Global Land Cover Layers—Collection 2. Remote Sens. 12, 1044. https://doi.org/10.3390/rs12061044
15. Cameron, G.J., Dang, H.-A.H., Dinc, M., Foster, J., Lokshin, M.M., 2019. Measuring the Statistical Capacity of Nation (No. 8693). World Bank, Washington, DC.
16. Campbell, G., Kuehl, H., N'Goran Kouamé, P., Boesch, C., 2008. Alarming decline of West African chimpanzees in Côte d'Ivoire. Curr. Biol. 18, R903–R904. https://doi.org/10.1016/j.cub.2008.08.015
17. Chazdon, R.L., Brancalion, P.H.S., Laestadius, L., Bennett-Curry, A., Buckingham, K., Kumar, C., Moll-Rocek, J., Vieira, I.C.G., Wilson, S.J., 2016. When is a forest a forest? Forest concepts and definitions in the era of forest and landscape restoration. Ambio 45, 538–550. https://doi.org/10.1007/s13280-016-0772-y
18. Chen, S., Woodcock, C.E., Bullock, E.L., Arévalo, P., Torchinava, P., Peng, S., Olofsson, P., 2021. Monitoring temperate forest degradation on Google Earth Engine using Landsat time series analysis. Remote Sens. Environ. 265, 112648. https://doi.org/10.1016/j.rse.2021.112648
19. Cohen, W.B., Yang, Z., Kennedy, R., 2010. Detecting trends in forest disturbance and recovery using yearly Landsat time series: 2. TimeSync — Tools for calibration and validation. Remote Sens. Environ. 114, 2911–2924. https://doi.org/10.1016/j.rse.2010.07.010
20. Crowther, T.W., Glick, H.B., Covey, K.R., Bettigole, C., Maynard, D.S., Thomas, S.M., Smith, J.R., Hintler, G., Duguid, M.C., Amatulli, G., Tuanmu, M.-N., Jetz, W., Salas, C., Stam, C., Piotto, D., Tavani, R., Green, S., Bruce, G., Williams, S.J., Wiser, S.K., Huber, M.O., Hengeveld, G.M., Nabuurs, G.-J., Tikhonova, E., Borchardt, P., Li, C.-F., Powrie, L.W., Fischer, M., Hemp, A., Homeier, J., Cho, P., Vibrans, A.C., Umunay, P.M., Piao, S.L., Rowe, C.W., Ashton, M.S., Crane, P.R., Bradford, M.A., 2015. Mapping tree density at a global scale. Nature 525, 201–205. https://doi.org/10.1038/nature14967
21. Dech, S., Holzwarth, S., Asam, S., Andresen, T., Bachmann, M., Boettcher, M., Dietz, A., Eisfelder, C., Frey, C., Gesell, G., Gessner, U., Hirner, A., Hofmann, M., Kirches, G., Klein, D., Klein, I., Kraus, T.,

Krause, D., Plank, S., Popp, T., Reinermann, S., Reiners, P., Roessler, S., Ruppert, T., Scherbachenko, A., Vignesh, R., Wolfmueller, M., Zwenzner, H., Kuenzer, C., 2021. Potential and Challenges of Harmonizing 40 Years of AVHRR Data: The TIMELINE Experience. Remote Sens. 13, 3618. https://doi.org/10.3390/rs13183618

22. Dimiceli, C., Carroll, M., Sohlberg, R., Kim, D., Townshend, J., 2015. MOD44B MODIS/terra vegetation continuous fields yearly L3 global 250m SIN grid V006. NASA EOSDIS Land Processes DAAC, Sioux Falls, USA.
23. Estoque, R.C., Dasgupta, R., Winkler, K., Avitabile, V., Johnson, B.A., Myint, S.W., Gao, Y., Ooba, M., Murayama, Y., Lasco, R.D., 2022. Spatiotemporal pattern of global forest change over the past 60 years and the forest transition theory. Environ. Res. Lett. 17, 084022. https://doi.org/10.1088/1748-9326/ac7df5
24. Estoque, R.C., Johnson, B.A., Gao, Y., DasGupta, R., Ooba, M., Togawa, T., Hijioka, Y., Murayama, Y., Gavina, L.D., Lasco, R.D., Nakamura, S., 2021. Remotely sensed tree canopy cover-based indicators for monitoring global sustainability and environmental initiatives. Environ. Res. Lett. 16. https://doi.org/10.1088/1748-9326/abe5d9
25. European Commission, 2022. Proposal for a REGULATION OF THE EUROPEAN PARLIAMENT AND OF THE COUNCIL on nature restoration. European Comission, Brussels.
26. FAO, 2020. Global Forest Resources Assessment 2020. FAO, Rome, Italy.
27. FAO, 2016. Global Forest Resources Assessment 2015. FAO, Rome, Italy.
28. FAO, 1998. Guidelines for the management of tropical forests 1. The production of wood (No. 135). FAO, Rome, Italy.
29. Ferrer Velasco, R., Köthke, M., Lippe, M., Günter, S., 2020. Scale and context dependency of deforestation drivers: Insights from spatial econometrics in the tropics. PLOS ONE 15, 1–32. https://doi.org/10.1371/journal.pone.0226830
30. FPA, 2017. State of the forests Tasmania 2017. Forest Practices Authority, Tasmania, Australia.
31. Friedlingstein, P., O'Sullivan, M., Jones, M.W., Andrew, R.M., Gregor, L., Hauck, J., Le Quéré, C., Luijkx, I.T., Olsen, A., Peters, G.P., Peters, W., Pongratz, J., Schwingshackl, C., Sitch, S., Canadell, J.G., Ciais, P., Jackson, R.B., Alin, S.R., Alkama, R., Arneth, A., Arora, V.K., Bates, N.R., Becker, M., Bellouin, N., Bittig, H.C., Bopp, L., Chevallier, F., Chini, L.P., Cronin, M., Evans, W., Falk, S., Feely, R.A., Gasser, T., Gehlen, M., Gkritzalis, T., Gloege, L., Grassi, G., Gruber, N., Gürses, Ö., Harris, I., Hefner, M., Houghton, R.A., Hurtt, G.C., Iida, Y., Ilyina, T., Jain, A.K., Jersild, A., Kadono, K., Kato, E., Kennedy, D., Klein Goldewijk,

K., Knauer, J., Korsbakken, J.I., Landschützer, P., Lefèvre, N., Lindsay, K., Liu, J., Liu, Z., Marland, G., Mayot, N., McGrath, M.J., Metzl, N., Monacci, N.M., Munro, D.R., Nakaoka, S.-I., Niwa, Y., O'Brien, K., Ono, T., Palmer, P.I., Pan, N., Pierrot, D., Pocock, K., Poulter, B., Resplandy, L., Robertson, E., Rödenbeck, C., Rodriguez, C., Rosan, T.M., Schwinger, J., Séférian, R., Shutler, J.D., Skjelvan, I., Steinhoff, T., Sun, Q., Sutton, A.J., Sweeney, C., Takao, S., Tanhua, T., Tans, P.P., Tian, X., Tian, H., Tilbrook, B., Tsujino, H., Tubiello, F., van der Werf, G.R., Walker, A.P., Wanninkhof, R., Whitehead, C., Willstrand Wranne, A., Wright, R., Yuan, W., Yue, C., Yue, X., Zaehle, S., Zeng, J., Zheng, B., 2022. Global Carbon Budget 2022. Earth Syst. Sci. Data 14, 4811–4900. https://doi.org/10.5194/essd-14-4811-2022

32. Gou, J., Wang, F., Jin, K., Mu, X., Chen, D., 2019. More realistic land-use and vegetation parameters in a regional climate model reduce model biases over China. Int. J. Climatol. 39, 4825–4837. https://doi.org/10.1002/joc.6110
33. Hansen, M.C., Potapov, P.V., Moore, R., Hancher, M., Turubanova, S.A., Tyukavina, A., Thau, D., Stehman, S.V., Goetz, S.J., Loveland, T.R., Kommareddy, A., Egorov, A., Chini, L., Justice, C.O., Townshend, J.R.G., 2013. High-Resolution Global Maps of 21st-Century Forest Cover Change. Science 342, 850–853. https://doi.org/10.1126/science.1244693
34. Harris, C.R., Millman, K.J., van der Walt, S.J., Gommers, R., Virtanen, P., Cournapeau, D., Wieser, E., Taylor, J., Berg, S., Smith, N.J., Kern, R., Picus, M., Hoyer, S., van Kerkwijk, M.H., Brett, M., Haldane, A., del Río, J.F., Wiebe, M., Peterson, P., Gérard-Marchant, P., Sheppard, K., Reddy, T., Weckesser, W., Abbasi, H., Gohlke, C., Oliphant, T.E., 2020. Array programming with NumPy. Nature 585, 357–362. https://doi.org/10.1038/s41586-020-2649-2
35. Hauhouot, A.A., 1992. Les ressources forestières dans la problématique du développement en Côte-d'lvoire. Espace Géographique 21, 357–365. https://doi.org/10.3406/spgeo.1992.3110
36. Herrera, D., Pfaff, A., Robalino, J., 2019. Impacts of protected areas vary with the level of government: Comparing avoided deforestation across agencies in the Brazilian Amazon. Proc. Natl. Acad. Sci. 116, 14916–14925. https://doi.org/10.1073/pnas.1802877116
37. Ioannidis, J.P.A., 2018. The Proposal to Lower P Value Thresholds to .005. JAMA 319, 1429–1430. https://doi.org/10.1001/jama.2018.1536
38. IPCC, 2022. Climate Change 2022: Impacts, Adaptation, and Vulnerability. Contribution of Working Group II to the Sixth Assessment Report of the Intergovernmental Panel on Climate Change.
39. Karger, D.N., Conrad, O., Böhner, J., Kawohl, T., Kreft, H., Soria-Auza, R.W., Zimmermann, N.E., Linder,

H.P., Kessler, M., 2017. Climatologies at high resolution for the earth's land surface areas. Sci. Data 4, 170122.

40. Kašpar, V., Hederová, L., Macek, M., Müllerová, J., Prošek, J., Surový, P., Wild, J., Kopecký, M., 2021. Temperature buffering in temperate forests: Comparing microclimate models based on ground measurements with active and passive remote sensing. Remote Sens. Environ. 263, 112522. https://doi.org/10.1016/j.rse.2021.112522
41. Kim, D.-H., Sexton, J.O., Noojipady, P., Huang, C., Anand, A., Channan, S., Feng, M., Townshend, J.R., 2014. Global, Landsat-based forest-cover change from 1990 to 2000. Remote Sens. Environ. 155, 178–193. https://doi.org/10.1016/j.rse.2014.08.017
42. Kouakou, A.C.A., Coulibaly, B., Kaba, D., Anoh, K.P., Courtin, F., 2018. Dynamique de peuplement et modification paysagère dans le parc national de la Marahoué (Côte d'Ivoire). Confl. Dyn. Paysages Sécurité Aliment. En Afr. Subsaharienne 36, 206–216.
43. Kovacs, K., West, G., Nowak, D.J., Haight, R.G., 2022. Tree cover and property values in the United States: A national meta-analysis. Ecol. Econ. 197, 107424. https://doi.org/10.1016/j.ecolecon.2022.107424
44. Krishnan, S., Wiederkehr Guerra, G., Bertrand, D., Wertz-Kanounnikoff, S., Kettle, C.J., 2020. The pollination services of forests - a review of forest and landscape interventions to enhance their cross-sectoral benefits (No. 15), Forestry Working Papers. FAO & Biodiversity International, Rome.
45. Kühl, H.S., Sop, T., Williamson, E.A., Mundry, R., Brugière, D., Campbell, G., Cohen, H., Danquah, E., Ginn, L., Herbinger, I., Jones, S., Junker, J., Kormos, R., Kouakou, C.Y., N'Goran, P.K., Normand, E., Shutt-Phillips, K., Tickle, A., Vendras, E., Welsh, A., Wessling, E.G., Boesch, C., 2017. The Critically Endangered western chimpanzee declines by 80%. Am. J. Primatol. 79, e22681. https://doi.org/10.1002/ajp.22681
46. Kuyper, J., Schroeder, H., Linnér, B.-O., 2018. The Evolution of the UNFCCC. Annu. Rev. Environ. Resour. 43, 343–368. https://doi.org/10.1146/annurev-environ-102017-030119
47. Lantz, V., McMonagle, G., Hennigar, C., Sharma, C., Withey, P., Ochuodho, T., 2022. Forest succession, management and the economy under a changing climate: Coupling economic and forest management models to assess impacts and adaptation options. For. Policy Econ. 142, 102781. https://doi.org/10.1016/j.forpol.2022.102781
48. Lawrence, P.J., Chase, T.N., 2007. Representing a new MODIS consistent land surface in the Community Land Model (CLM 3.0). J. Geophys. Res. Biogeosciences 112. https://doi.org/10.1029/2006JG000168
49. Lee, S., Lee, R.J., Scherr, S., 2023. How tree canopy cover can reduce urban suicide attempts: A geospatial

analysis of the moderating role of area deprivation. Landsc. Urban Plan. 230, 104606. https://doi.org/10.1016/j.landurbplan.2022.104606

50. Lehmann, E.A., Caccetta, P., Lowell, K., Mitchell, A., Zhou, Z.-S., Held, A., Milne, T., Tapley, I., 2015. SAR and optical remote sensing: Assessment of complementarity and interoperability in the context of a large-scale operational forest monitoring system. Remote Sens. Environ. 156, 335–348. https://doi.org/10.1016/j.rse.2014.09.034
51. Li, X., Zhou, Y., Zhao, M., Zhao, X., 2020. A harmonized global nighttime light dataset 1992–2018. Sci. Data 7, 168. https://doi.org/10.1038/s41597-020-0510-y
52. Lucas, R., Mueller, N., Siggins, A., Owers, C., Clewley, D., Bunting, P., Kooymans, C., Tissott, B., Lewis, B., Lymburner, L., Metternicht, G., 2019. Land Cover Mapping using Digital Earth Australia. Data 4. https://doi.org/10.3390/data4040143
53. Luyssaert, S., Schulze, E.-D., Börner, A., Knohl, A., Hessenmöller, D., Law, B.E., Ciais, P., Grace, J., 2008. Old-growth forests as global carbon sinks. Nature 455, 213–215. https://doi.org/10.1038/nature07276
54. Mackey, B., Cadman, S., Rogers, N., Hugh, S., 2017. Assessing the risk to the conservation status of temperate rainforest from exposure to mining, commercial logging, and climate change: A Tasmanian case study. Biol. Conserv. 215, 19–29. https://doi.org/10.1016/j.biocon.2017.08.032
55. Maes, J., Bruzón, A.G., Barredo, J.I., Vallecillo, S., Vogt, P., Rivero, I.M., Santos-Martín, F., 2023. Accounting for forest condition in Europe based on an international statistical standard. Nat. Commun. 14, 3723. https://doi.org/10.1038/s41467-023-39434-0
56. MapBiomas, 2021. MapBiomas Alert Project V4.0 - Validation and Refinement System for Deforestation Alerts with High Resolution Images.
57. Maraun, D., Knevels, R., Mishra, A.N., Truhetz, H., Bevacqua, E., Proske, H., Zappa, G., Brenning, A., Petschko, H., Schaffer, A., Leopold, P., Puxley, B.L., 2022. A severe landslide event in the Alpine foreland under possible future climate and land-use changes. Commun. Earth Environ. 3, 87. https://doi.org/10.1038/s43247-022-00408-7
58. Mazón, M.M., Klanderud, K., Finegan, B., Veintimilla, D., Bermeo, D., Murrieta, E., Delgado, D., Sheil, D., 2020. How forest structure varies with elevation in old growth and secondary forest in Costa Rica. For. Ecol. Manag. 469, 118191. https://doi.org/10.1016/j.foreco.2020.118191
59. McDowell, N.G., Allen, C.D., Anderson-Teixeira, K., Aukema, B.H., Bond-Lamberty, B., Chini, L., Clark, J.S., Dietze, M., Grossiord, C., Hanbury-Brown, A., Hurtt, G.C., Jackson, R.B., Johnson, D.J., Kueppers, L.,

Lichstein, J.W., Ogle, K., Poulter, B., Pugh, T.A.M., Seidl, R., Turner, M.G., Uriarte, M., Walker, A.P., Xu, C., 2020. Pervasive shifts in forest dynamics in a changing world. Science 368, eaaz9463. https://doi.org/10.1126/science.aaz9463

60. Michael Mills, 2017. The special birds of Angola. Go-Away-Birding, Cape Town, South Africa.
61. Mohammad, A.G., Adam, M.A., 2010. The impact of vegetative cover type on runoff and soil erosion under different land uses. CATENA 81, 97–103. https://doi.org/10.1016/j.catena.2010.01.008
62. Montibeller, B., Kmoch, A., Virro, H., Mander, Ü., Uuemaa, E., 2020. Increasing fragmentation of forest cover in Brazil's Legal Amazon from 2001 to 2017. Sci. Rep. 10, 5803. https://doi.org/10.1038/s41598-020-62591-x
63. Nesha, M.K., Herold, M., De Sy, V., Duchelle, A.E., Martius, C., Branthomme, A., Garzuglia, M., Jonsson, O., Pekkarinen, A., 2021. An assessment of data sources, data quality and changes in national forest monitoring capacities in the Global Forest Resources Assessment 2005–2020. Environ. Res. Lett. 16. https://doi.org/10.1088/1748-9326/abd81b
64. Nicolson, M., 1996. Humboldtian Plant Geography after Humboldt: The Link to Ecology. Br. J. Hist. Sci. 29, 289–310.
65. Pedregosa, F., Varoquaux, G., Gramfort, A., Michel, V., Thirion, B., Grisel, O., Blondel, M., Prettenhofer, P., Weiss, R., Dubourg, V., Vanderplas, J., Passos, A., Cournapeau, D., Brucher, M., Perrot, M., Duchesnay, É., 2011. Scikit-learn: Machine Learning in Python. J. Mach. Learn. Res. 12, 2825–2830.
66. Pillay, R., Venter, M., Aragon-Osejo, J., González-del-Pliego, P., Hansen, A.J., Watson, J.E., Venter, O., 2022. Tropical forests are home to over half of the world's vertebrate species. Front. Ecol. Environ. 20, 10–15. https://doi.org/10.1002/fee.2420
67. Qin, Y., Xiao, X., Wigneron, J.-P., Ciais, P., Brandt, M., Fan, L., Li, X., Crowell, S., Wu, X., Doughty, R., Zhang, Y., Liu, F., Sitch, S., Moore, B., 2021. Carbon loss from forest degradation exceeds that from deforestation in the Brazilian Amazon. Nat. Clim. Change 11, 442–448. https://doi.org/10.1038/s41558-021-01026-5
68. Radwan, T.M., Blackburn, G.A., Whyatt, J.D., Atkinson, P.M., 2021. Global land cover trajectories and transitions. Sci. Rep. 11, 12814. https://doi.org/10.1038/s41598-021-92256-2
69. Remelgado, R., Conrad, C., Meyer, C., 2023. Limitations in historical satellite archives bias SDG monitoring. preprint. https://doi.org/10.31223/X5QH37
70. Rizayeva, A., Nita, M.D., Radeloff, V.C., 2023. Large-area, 1964 land cover classifications of Corona spy

satellite imagery for the Caucasus Mountains. Remote Sens. Environ. 284, 113343. https://doi.org/10.1016/j.rse.2022.113343

71. Roberts, D.R., Bahn, V., Ciuti, S., Boyce, M.S., Elith, J., Guillera-Arroita, G., Hauenstein, S., Lahoz-Monfort, J.J., Schröder, B., Thuiller, W., Warton, D.I., Wintle, B.A., Hartig, F., Dormann, C.F., 2017. Cross-validation strategies for data with temporal, spatial, hierarchical, or phylogenetic structure. Ecography 40, 913–929. https://doi.org/10.1111/ecog.02881
72. Rosa, I.M.D., Purves, D., Souza, C., Jr, Ewers, R.M., 2013. Predictive Modelling of Contagious Deforestation in the Brazilian Amazon. PLOS ONE 8, 1–14. https://doi.org/10.1371/journal.pone.0077231
73. Santoro, M., Kirches, G., Wevers, J., Boettcher, M., Brockmann, C., Lamarche, C., Bontemps, S., Moreau, I., Defourny, P., 2017. Land Cover CCI - Product User Guide Version 2.0.
74. Satopaa, V., Albrecht, J., Irwin, D., Raghavan, B., 2011. Finding a “Kneedle” in a Haystack: Detecting Knee Points in System Behavior, in: 2011 31st International Conference on Distributed Computing Systems Workshops. pp. 166–171. https://doi.org/10.1109/ICDCSW.2011.20
75. Schröder, J.M., Rodríguez, L.P.Á., Günter, S., 2021. Research trends: Tropical dry forests: The neglected research agenda? For. Policy Econ. 122, 102333. https://doi.org/10.1016/j.forpol.2020.102333
76. Schwaab, J., Meier, R., Mussetti, G., Seneviratne, S., Bürgi, C., Davin, E.L., 2021. The role of urban trees in reducing land surface temperatures in European cities. Nat. Commun. 12, 6763. https://doi.org/10.1038/s41467-021-26768-w
77. Seckler, H., Metzler, R., 2022. Bayesian deep learning for error estimation in the analysis of anomalous diffusion. Nat. Commun. 13, 6717. https://doi.org/10.1038/s41467-022-34305-6
78. Seidl, R., Schelhaas, M.-J., Rammer, W., Verkerk, P.J., 2014. Increasing forest disturbances in Europe and their impact on carbon storage. Nat. Clim. Change 4, 806–810. https://doi.org/10.1038/nclimate2318
79. Selbig, W.R., Loheide II, S.P., Shuster, W., Scharenbroch, B.C., Coville, R.C., Kruegler, J., Avery, W., Haefner, R., David Nowak, 2022. Loss of street tree canopy increases stormwater runoff (Report No. 2022–3074), Fact Sheet. Reston, VA. https://doi.org/10.3133/fs20223074
80. Senf, C., Pflugmacher, D., Zhiqiang, Y., Sebald, J., Knorn, J., Neumann, M., Hostert, P., Seidl, R., 2018. Canopy mortality has doubled in Europe’s temperate forests over the last three decades. Nat. Commun. 9, 4978. https://doi.org/10.1038/s41467-018-07539-6
81. Senf, C., Seidl, R., 2021. Mapping the forest disturbance regimes of Europe. Nat. Sustain. 4, 63–70. https://doi.org/10.1038/s41893-020-00609-y

82. Sexton, J.O., Song, X.-P., Feng, M., Noojipady, P., Anand, A., Huang, C., Kim, D.-H., Collins, K.M., Channan, S., DiMiceli, C., Townshend, J.R., 2013. Global, 30-m resolution continuous fields of tree cover: Landsat-based rescaling of MODIS vegetation continuous fields with lidar-based estimates of error. Int. J. Digit. Earth 6, 427–448. https://doi.org/10.1080/17538947.2013.786146
83. Shapiro, A.C., Bernhard, K.P., Zenobi, S., Müller, D., Aguilar-Amuchastegui, N., d'Annunzio, R., 2021. Proximate Causes of Forest Degradation in the Democratic Republic of the Congo Vary in Space and Time. Front. Conserv. Sci. 2. https://doi.org/10.3389/fcosc.2021.690562
84. Sommerfeld, A., Senf, C., Buma, B., D'Amato, A.W., Després, T., Díaz-Hormazábal, I., Fraver, S., Frelich, L.E., Gutiérrez, Á.G., Hart, S.J., Harvey, B.J., He, H.S., Hlásny, T., Holz, A., Kitzberger, T., Kulakowski, D., Lindenmayer, D., Mori, A.S., Müller, J., Paritsis, J., Perry, G.L.W., Stephens, S.L., Svoboda, M., Turner, M.G., Veblen, T.T., Seidl, R., 2018. Patterns and drivers of recent disturbances across the temperate forest biome. Nat. Commun. 9, 4355. https://doi.org/10.1038/s41467-018-06788-9
85. Song, X.-P., Hansen, M.C., Stehman, S.V., Potapov, P.V., Tyukavina, A., Vermote, E.F., Townshend, J.R., 2018. Global land change from 1982 to 2016. Nature 560, 639–643. https://doi.org/10.1038/s41586-018-0411-9
86. Song, X.-P., Huang, C., Feng, M., Sexton, J.O., Channan, S., Townshend, J.R., 2014. Integrating global land cover products for improved forest cover characterization: an application in North America. Int. J. Digit. Earth 7, 709–724. https://doi.org/10.1080/17538947.2013.856959
87. Soranno, P.A., Cheruvelil, K.S., Bissell, E.G., Bremigan, M.T., Downing, J.A., Fergus, C.E., Filstrup, C.T., Henry, E.N., Lottig, N.R., Stanley, E.H., Stow, C.A., Tan, P.-N., Wagner, T., Webster, K.E., 2014. Cross-scale interactions: quantifying multi-scaled cause–effect relationships in macrosystems. Front. Ecol. Environ. 12, 65–73. https://doi.org/10.1890/120366
88. Stevens, V.M., Whitmee, S., Le Galliard, J.-F., Clobert, J., Böhning-Gaese, K., Bonte, D., Brändle, M., Matthias Dehling, D., Hof, C., Trochet, A., Baguette, M., 2014. A comparative analysis of dispersal syndromes in terrestrial and semi-terrestrial animals. Ecol. Lett. 17, 1039–1052. https://doi.org/10.1111/ele.12303
89. Stibig, H.-J., Achard, F., Carboni, S., Raši, R., Miettinen, J., 2014. Change in tropical forest cover of Southeast Asia from 1990 to 2010. Biogeosciences 11, 247–258. https://doi.org/10.5194/bg-11-247-2014
90. Taha, A.A., Hanbury, A., 2015. Metrics for evaluating 3D medical image segmentation: analysis, selection, and tool. BMC Med. Imaging 15, 29. https://doi.org/10.1186/s12880-015-0068-x

91. Tang, H., Armston, J., Hancock, S., Marselis, S., Goetz, S., Dubayah, R., 2019. Characterizing global forest canopy cover distribution using spaceborne lidar. Remote Sens. Environ. 231, 111262. https://doi.org/10.1016/j.rse.2019.111262
92. Taubert, F., Fischer, R., Groeneveld, J., Lehmann, S., Müller, M.S., Rödig, E., Wiegand, T., Huth, A., 2018. Global patterns of tropical forest fragmentation. Nature 554, 519.
93. Thom, D., Seidl, R., 2016. Natural disturbance impacts on ecosystem services and biodiversity in temperate and boreal forests. Biol. Rev. 91, 760–781. https://doi.org/10.1111/brv.12193
94. Trancoso, R., 2021. Changing Amazon deforestation patterns: urgent need to restore command and control policies and market interventions. Environ. Res. Lett. 16, 041004. https://doi.org/10.1088/1748-9326/abee4c
95. Tsendbazar, N., Herold, M., Li, L., Tarko, A., Bruin, S. de, Masiliunas, D., Lesiv, M., Fritz, S., Buchhorn, M., Smets, B., Kerchove, R.V.D., Duerauer, M., 2021. Towards operational validation of annual global land cover maps. Remote Sens. Environ. 266, 112686. https://doi.org/10.1016/j.rse.2021.112686
96. UCB, 2012. Global Administrative Areas [WWW Document]. URL www.gadm.org (accessed 10.14.19).
97. UNFCCC, 2015. Adoption of the Paris Agreement, 21st Conference of the Parties.
98. Vancutsem, C., Achard, F., Pekel, J.-F., Vieilledent, G., Carboni, S., Simonetti, D., Gallego, J., Aragão, L.E.O.C., Nasi, R., 2021. Long-term (1990-2019) monitoring of forest cover changes in the humid tropics. Sci. Adv. 7, eabe1603. https://doi.org/10.1126/sciadv.abe1603
99. Walker, X.J., Baltzer, J.L., Cumming, S.G., Day, N.J., Ebert, C., Goetz, S., Johnstone, J.F., Potter, S., Rogers, B.M., Schuur, E.A.G., Turetsky, M.R., Mack, M.C., 2019. Increasing wildfires threaten historic carbon sink of boreal forest soils. Nature 572, 520–523. https://doi.org/10.1038/s41586-019-1474-y
100. Wang, J., Yang, D., Detto, M., Nelson, B.W., Chen, M., Guan, K., Wu, S., Yan, Z., Wu, J., 2020. Multi-scale integration of satellite remote sensing improves characterization of dry-season green-up in an Amazon tropical evergreen forest. Remote Sens. Environ. 246, 111865. https://doi.org/10.1016/j.rse.2020.111865
101. Wang, S.-H., Pillai, H.S., Wang, S., Achenie, L.E.K., Xin, H., 2021. Infusing theory into deep learning for interpretable reactivity prediction. Nat. Commun. 12, 5288. https://doi.org/10.1038/s41467-021-25639-8
102. WMO, 2022. The 2022 GCOS ECVs Requirements (GCOS 245). World Meteorological Organization, Geneva, Switzerland.
103. World Bank, 2019. Environment and Renewable Natural Resources in Angola - Opportunities to Diversify the National Economy, Generate Income for local communities, enhance environmental management capacity and build resilience to climate change. World Bank, Washington, D.C., USA.

104. Wulder, M.A., Hermosilla, T., Stinson, G., Gougeon, F.A., White, J.C., Hill, D.A., Smiley, B.P., 2020. Satellite-based time series land cover and change information to map forest area consistent with national and international reporting requirements. For. Int. J. For. Res. 93, 331–343. https://doi.org/10.1093/forestry/cpaa006

105. Wulder, M.A., White, J.C., Loveland, T.R., Woodcock, C.E., Belward, A.S., Cohen, W.B., Fosnight, E.A., Shaw, J., Masek, J.G., Roy, D.P., 2016. The global Landsat archive: Status, consolidation, and direction. Remote Sens. Environ. 185, 271–283. https://doi.org/10.1016/j.rse.2015.11.032

106. Xu, L., Shi, Y., Fang, H., Zhou, G., Xu, X., Zhou, Y., Tao, J., Ji, B., Xu, J., Li, C., Chen, L., 2018. Vegetation carbon stocks driven by canopy density and forest age in subtropical forest ecosystems. Sci. Total Environ. 631–632, 619–626. https://doi.org/10.1016/j.scitotenv.2018.03.080

107. Xu, X., Medvigy, D., Trugman, A.T., Guan, K., Good, S.P., Rodriguez-Iturbe, I., 2018. Tree cover shows strong sensitivity to precipitation variability across the global tropics. Glob. Ecol. Biogeogr. 27, 450–460. https://doi.org/10.1111/geb.12707

108. Yamazaki, D., Ikeshima, D., Tawatari, R., Yamaguchi, T., O'Loughlin, F., Neal, J.C., Sampson, C.C., Kanae, S., Bates, P.D., 2017. A high-accuracy map of global terrain elevations. Geophys. Res. Lett. 44, 5844–5853. https://doi.org/10.1002/2017GL072874

109. Zhao, S., Liu, S., Li, Z., Sohl, T., 2010. A spatial resolution threshold of land cover in estimating terrestrial carbon sequestration in four counties in Georgia and Alabama, USA. Biogeosciences 7. https://doi.org/10.5194/bg-7-71-2010

SUPPLEMENTARY INFORMATION

Table 1. Model predictors. Listing of variables used to predict canopy densities. as well as the respective data sources, temporal coverage, and spatial and temporal resolution. The column "reasoning" summarises the thought process behind the selection of each variable.

predictor	dataset	source	period	spatial res.	temporal res.	reasoning
Country	GADM[52]					Controls for the influence of national governance
Forest density					annual	Expected future outcome of persistent gains/losses
Mean year of change				300-m		Long-term trends inform on the tendency for persistent loss
Density of changes	GFC[32]	Hansen et al.	2000-2020		multi-year aggregate	
Mean year of change				5-km		Controls for spillover effects
Density of changes						
Land cover	CCILC[44]		1992-2020	300-m		e.g. higher deforestation are more likely under agriculture than under dense tree cover
Light intensity	NTL[51]		1992-2018	1-km	annual	The existence and intensity of human activity drive deforestation
Tree cover density						
Short vegetation density						Year-specific data on vegetation cover occurrence and density
Non-vegetated surface density						
Tree cover density change	AVHRR-VCF[45]	Song et al.	1982-2016	5-km	annual	
Short vegetation density change						Direct information on sub-regional, long-term trends
Non-vegetated surface density change						
Elevation	MERIT DEM[47]	Yamazaki et al			snapshot	Changes are more common at low altitudes and over flat terrain
Slope						
Aridity	CHELSA[48]	-	1979-2018	1-km	multi-year aggregate	e.g. moist regions motivate extensive deforestation in favor of agricultural expansion
Precipitation						
Tree cover mismatch (1)	GFC and AVHRR-VCF		2000-2016	5-km		
Tree cover mismatch (2)	GFC and CCILC	-		5-km	annual	Controls for competing perceptions on the extent and density of forest cover given by different datasets
Tree cover mismatch (3)	CCILC and AVHRR-VCF		1992-2016	5-km		
Temporal distance	-	-	-	300-m	-	Time-fixed effect, controlling for the temporal distance between the mapping year and the nearest GFC data point

Table 2. CCI land cover tree-canopy fractions. Tree-canopy cover for each land cover class in the CCILC dataset, assuming the central percentage value of the range of possible values indicated in the class label (cf ref (Song et al., 2014)).

Land cover class	Forest cover (%)
Cropland, rainfed	
Herbaceous cover	
Tree or shrub cover	
Cropland, irrigated or post-flooding	
Mosaic cropland (>50%) / natural vegetation (tree, shrub, herbaceous cover) (<50%)	8.3
Mosaic natural vegetation (tree, shrub, herbaceous cover) (>50%) / cropland (<50%)	25
Tree cover, broadleaved, evergreen, closed to open (>15%)	100
Tree cover, broadleaved, deciduous, closed to open (>15%)	100
Tree cover, broadleaved, deciduous, closed (>40%)	100
Tree cover, broadleaved, deciduous, open (15-40%)	100
Tree cover, needleleaved, evergreen, closed to open (>15%)	100
Tree cover, needleleaved, evergreen, closed (>40%)	100
Tree cover, needleleaved, evergreen, open (15-40%)	100
Tree cover, needleleaved, deciduous, closed to open (>15%)	100
Tree cover, needleleaved, deciduous, closed (>40%)	100
Tree cover, needleleaved, deciduous, open (15-40%)	100
Tree cover, mixed leaf type (broadleaved and needleleaved)	100
Mosaic tree and shrub (>50%) / herbaceous cover (<50%)	37.5
Mosaic herbaceous cover (>50%) / tree and shrub (<50%)	12.5
Shrubland	
Shrubland evergreen	
Shrubland deciduous	
Grassland	
Lichens and mosses	
Sparse vegetation (tree, shrub, herbaceous cover) (<15%)	
Sparse tree (<15%)	
Sparse shrub (<15%)	
Sparse herbaceous cover (<15%)	
Tree cover, flooded, fresh or brakish water	100
Tree cover, flooded, saline water	100
Shrub or herbaceous cover, flooded, fresh/saline/brakish water	
Urban areas	
Bare areas	
Consolidated bare areas	
Unconsolidated bare areas	
Water bodies	
Permanent snow and ice	

Table 3. Continental correlations compared to national statistics. RMSE (in 1Mha) and r^2 for the year 2000, comparing treescape extents mapped by the GFC and by our data product against forest extents reported in national FRAs. The values derived with our data product are accompanied by uncertainty bounds based on the upper and lower confidence intervals surrounding the mean model predictions. We derived these metrics for each continent. In addition, we estimated the proportion of the total FRA area that the estimated RMSE corresponds to.

	FRA forest area	*r^2*		*RMSE*		*RMSE as a % of the FRA forest area*	
		GTCCC	GFC	TCCC	GFC	TCCC	GFC
Africa	658.18	0.80 (±0.00)	0.80	22.61 (±0.01)	11.43	3.46 (±0.41)	1.67
Americas	1615.36	0.97 (±0.00)	0.97	79.28 (±0.28)	29.88	4.92 (±0.32)	1.82
Asia	570.46	0.89 (±0.00)	0.89	33.91 (±0.07)	19.63	5.96 (±0.70)	3.55
Europe	956.7	0.98 (±0.00)	0.98	92.07 (±0.20)	72.97	9.63 (±0.18)	7.67
Oceania	180.81	0.95 (±0.00)	0.95	10.42 (±0.18)	47.53	5.76 (±0.25)	26.36

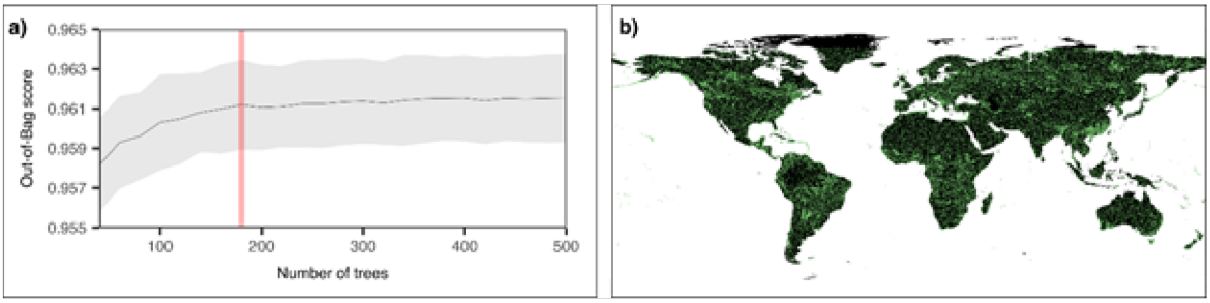

Figure 1 – Model training. Panel a) illustrates the selection of an optimal number of trees with which to train our Random Forest Regression model (RFReg). The centre dark line shows the mean Out-of-Bag (OOB) performance for each tested forest size, and the circumventing grey areas depict the standard deviation around the mean. The red vertical line shows the optimal forest size of 180 trees which we selected using knee detection. Note that the knee occurred when OOB performances stopped increasing notably. Panel b) shows the distribution of samples used to train our RFReg model. The green dots represent 78,135 unique sample locations within which we collected 625,080 samples across an 8-year period.

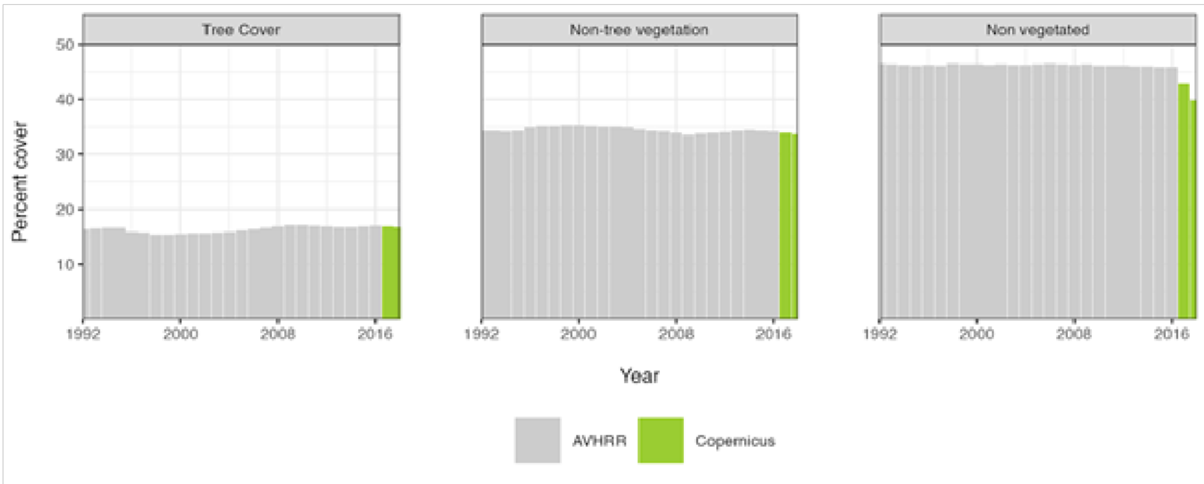

Figure 2 – Temporal stability of VCF predictions. Global percent cover of each VCF class between 1992 and 2018. Grey bars depict values obtained through the AVHRR-VCF, while green bars represent values obtained from the predicted VCF data. We see how the predictions of tree cover and non-tree vegetation are in line with global trends. However, predictions of non-vegetated cover deviate visibly.

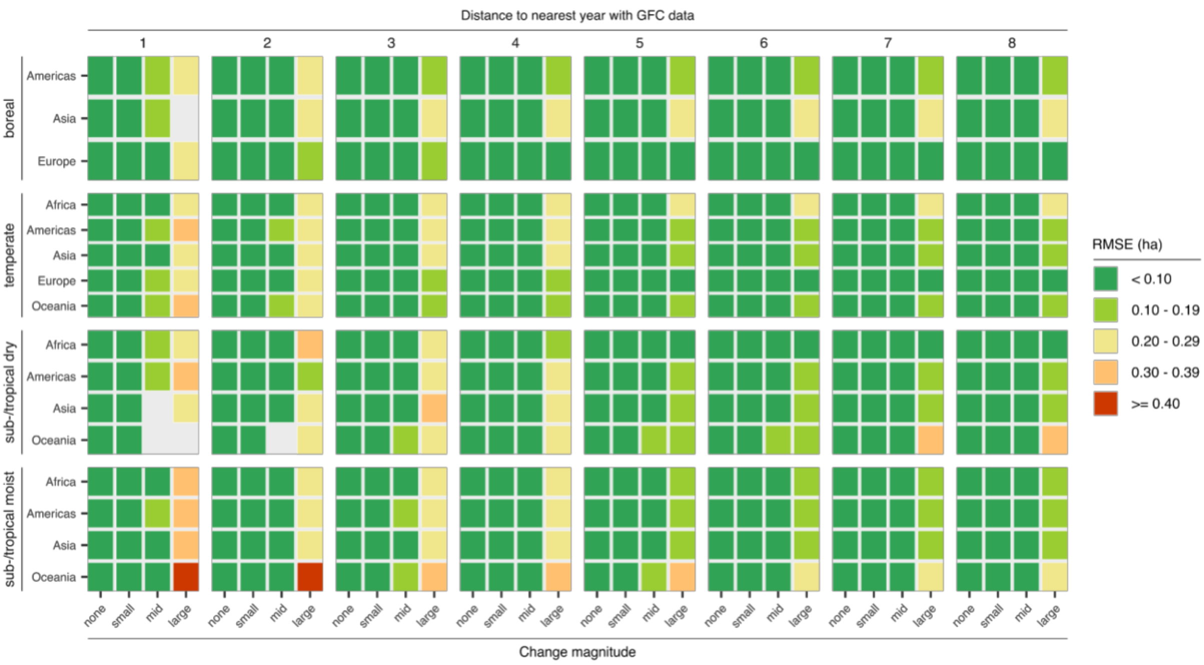

Supplementary Figure 3 – Uncertainty of quality assessment. Confidence interval of the RMSE for each continent, biome, and change magnitude (discriminated below), for different temporal gap sizes between the focal mapping year and the nearest year with reference data on tree-canopy cover (shown above). This plot is supplementary to Fig. 2, which displays the corresponding RMSE values.di.

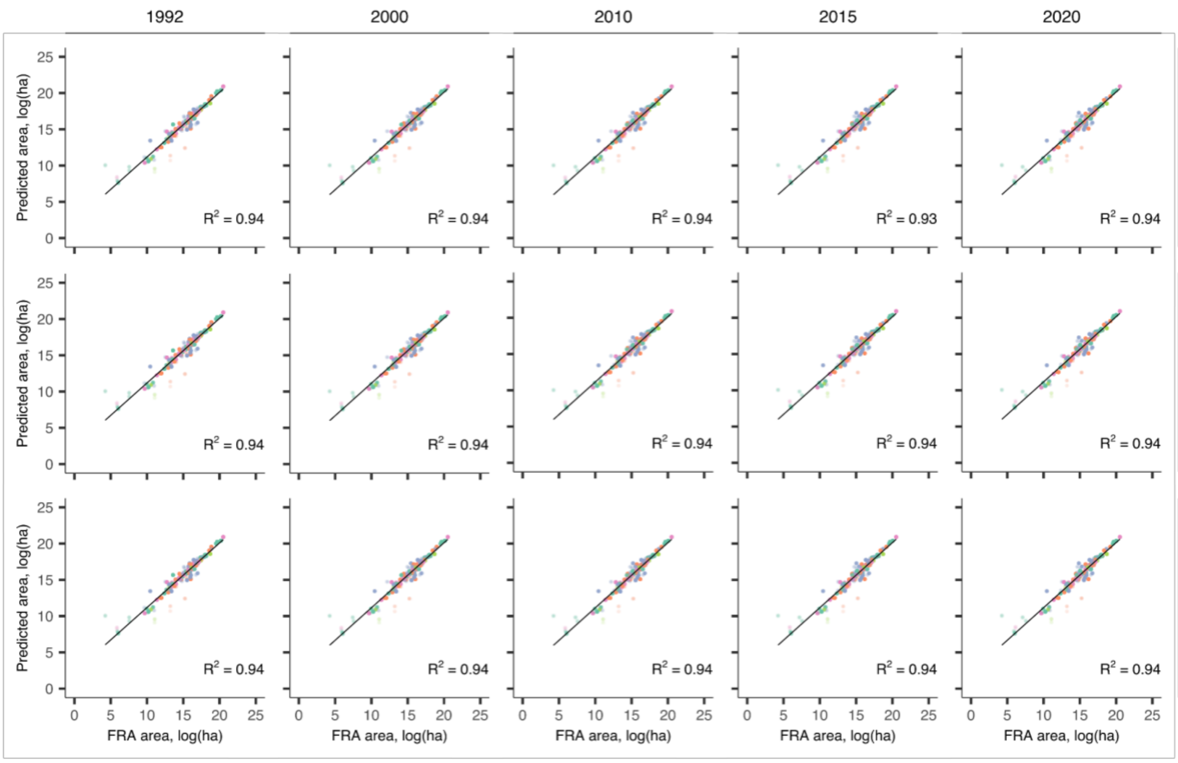

Figure 4 – Extended comparison with national statistics. Each plot shows the correlation between forest area reported in the Forest Resource Assessments (FRAs) and tree-canopy cover predicted by the presented GTCCC product. We ran this analysis for each FRA assessment year (each column, distinguished above), and repeated it for the mean pixel predictions and the upper and lower bounds of its 95% confidence interval (each row, distinguished on the right). The colours of each point indicate the continent each country belongs to (see in Fig. 3), and faded colours indicate uncertainties regarding the quality of national statistics. Our results show our predictions are consistent across FRA years and that correlations are robust to uncertainty in the GTCCC predictions. R^2 values were 0.94 for every iteration.

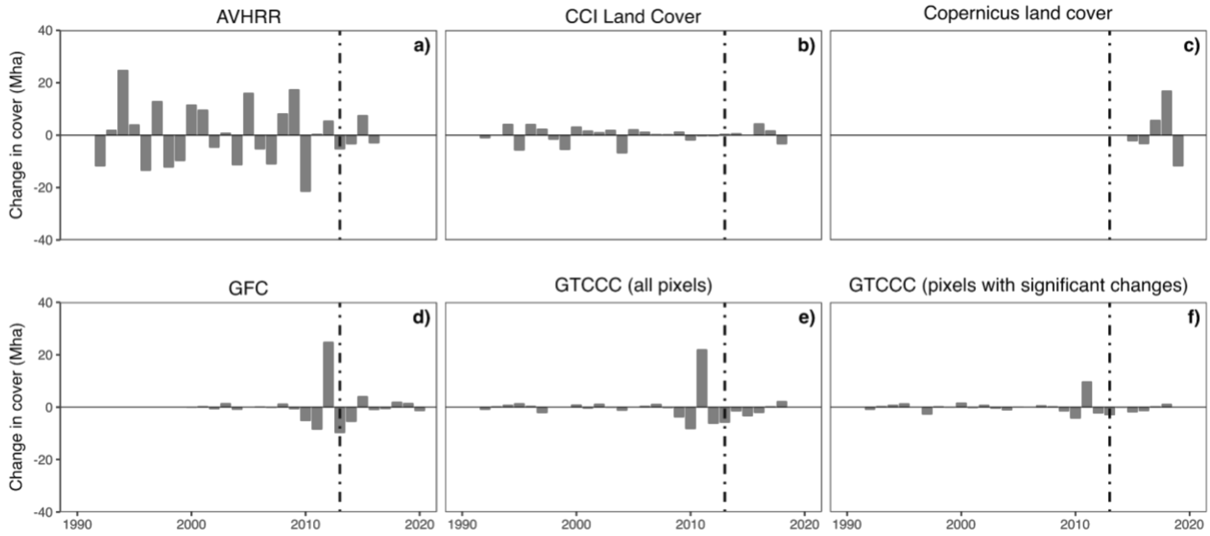

Figure 5. Time series consistency. Positive/negative outliers in year-to-year changes in cover (expressed in Mha) relative to the smoothed trend (constructed with LOWESS and a span of 0.5). Each panel shows this variable for each of the datasets contributing to our data product (**a-d**), namely AVHRR (**a**), CCI land cover (**b**), Copernicus land cover (**c**, used to extend the AVHRR time-series past 2016), and GFC (**d**). In addition, we applied the same analysis to our data before (**e**) and after (**f**) detecting significant changes using the Mann-Kendall test. The dashed vertical line highlights 2013, when Landsat 8 was launched, and which marks a substantial improvement in the frequency and quality of the Landsat data the GFC is based on (i.e., our reference data and sample source). The plot shows that our product (**e**) preserves anomalies visible in the GFC between 2010 and 2013 (**d**), corresponding to the period when Landsat 5 was decommissioned, leaving Landsat 7 as the only source of data despite its heavy degradation. However, the magnitude of these anomalies appears smaller in our data. When limiting our focus to pixels with significant changes (p-value < 0.0005) identified through the Mann-Kendall test, the prevalence of anomalies is reduced further. Note that despite integrating coarse-resolution (**a**), categorical (**b**), and contemporary data (**e**) to build our predictive model, their year-to-year anomalies are not replicated in our data.